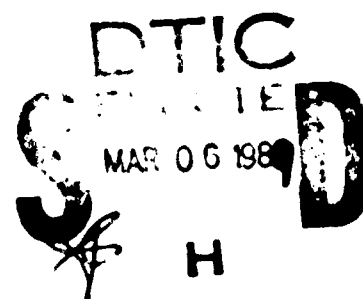


NAVAL POSTGRADUATE SCHOOL

Monterey, California

AD-A204 844



THESIS

THE VARIABILITY OF THE MARINE ATMOSPHERIC BOUNDARY LAYER
IN THE GREENLAND SEA MARGINAL ICE ZONE:
A CASE STUDY

by

Karl L. Dinkler

December, 1985

Thesis Advisor

K. L. Davidson

Approved for public release; distribution is unlimited.

89 3 06 011

Unclassified

security classification of this page

REPORT DOCUMENTATION PAGE

1a Report Security Classification Unclassified			1b Restrictive Markings		
2a Security Classification Authority			3 Distribution Availability of Report		
2b Declassification Downgrading Schedule			Approved for public release; distribution is unlimited.		
4 Performing Organization Report Number(s)			5 Monitoring Organization Report Number(s)		
6a Name of Performing Organization Naval Postgraduate School		6b Office Symbol (if applicable) 35	7a Name of Monitoring Organization Naval Postgraduate School		
6c Address (city, state, and ZIP code) Monterey, CA 93943-5000			7b Address (city, state, and ZIP code) Monterey, CA 93943-5000		
8a Name of Funding Sponsoring Organization		8b Office Symbol (if applicable)	9 Procurement Instrument Identification Number		
8c Address (city, state, and ZIP code)			10 Source of Funding Numbers		
			Program Element No Project No Task No Work Unit Accession No		
11 Title (include security classification) THE VARIABILITY OF THE MARINE ATMOSPHERIC BOUNDARY LAYER IN THE GREENLAND SEA MARGINAL ICE ZONE-- A CASE STUDY					
12 Personal Author(s) Karl L. Dinkler					
13a Type of Report Master's Thesis		13b Time Covered From To		14 Date of Report (year, month, day) December, 1988	
				15 Page Count 66	
16 Supplementary Notation The views expressed in this thesis are those of the author and do not reflect the official policy or position of the Department of Defense or the U.S. Government.					
17 Cosati Codes			18 Subject Terms (continue on reverse if necessary and identify by block number)		
Field	Group	Subgroup	marginal ice zone, Arctic boundary layer, vertical structure		
19 Abstract (continue on reverse if necessary and identify by block number)					
<p>The vertical structure of the atmospheric boundary layer in the East Greenland Sea Fram Strait marginal ice zone (MIZ) is examined for various wind flow regimes with respect to the ice edge. Rawinsonde profiles and surface observations collected from three ships during MIZEX-87 (20 March - 11 April 1987) served as the data set for the examination.</p> <p>Three specific flow regimes are discussed: on-ice flow, off-ice flow, and flow parallel to the ice. On-ice flow resulted in deep, moist mixed layers capped by high weak inversions at the MIZ. Off-ice flow resulted in multiple surface and elevated inversions, with specific humidity highest within an elevated lower-tropospheric layer and dry regions near the surface and aloft. Parallel flow led to the development of strikingly different boundary layer regimes separated by the ice edge: Over ice, deep surface and elevated inversions were associated with alternating moist and dry layers in the lower troposphere; over water, multiple elevated inversions were associated with an elevated lower-tropospheric moist layer and dry regions near the surface and aloft. Possible physical processes important for the development of the observed features are discussed.</p>					
20 Distribution Availability of Abstract			21 Abstract Security Classification		
<input checked="" type="checkbox"/> unclassified unlimited <input type="checkbox"/> same as report <input type="checkbox"/> DTIC users			Unclassified		
22a Name of Responsible Individual K. L. Davidson			22b Telephone (include Area code) (408) 646-3430		22c Office Symbol 63Sr

DD FORM 1473, 84 MAR

83 APR edition may be used until exhausted
All other editions are obsolete

security classification of this page

Unclassified

Approved for public release; distribution is unlimited.

The Variability of the Marine Atmospheric Boundary Layer
in the Greenland Sea Marginal Ice Zone-- A Case Study

by

Karl L. Dinkler
Lieutenant, United States Navy
BS, University of Florida, 1983

Submitted in partial fulfillment of the
requirements for the degree of

MASTER OF SCIENCE IN METEOROLOGY AND OCEANOGRAPHY

from the

NAVAL POSTGRADUATE SCHOOL
December, 1988

Author:

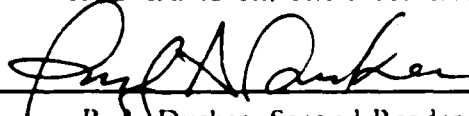


Karl L. Dinkler

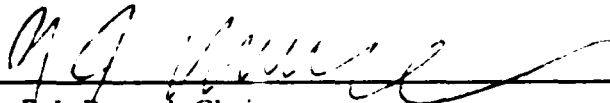
Approved by:



K. L. Davidson, Thesis Advisor



P. A. Durkee, Second Reader



R.J. Renard, Chairman,
Department of Meteorology



Gordon E. Schacher,
Dean of Science and Engineering

ABSTRACT

The vertical structure of the atmospheric boundary layer in the East Greenland Sea/Fram Strait marginal ice zone (MIZ) is examined for various wind flow regimes with respect to the ice edge. Rawinsonde profiles and surface observations collected from three ships during MIZEX-87 (20 March - 11 April 1987) served as the data set for the examination.

Three specific flow regimes are discussed: on-ice flow, off-ice flow, and flow parallel to the ice. On-ice flow resulted in deep, moist mixed layers capped by high weak inversions at the MIZ. Off-ice flow resulted in multiple surface and elevated inversions, with specific humidity highest within an elevated lower-tropospheric layer and dry regions near the surface and aloft. Parallel flow led to the development of strikingly different boundary layer regimes separated by the ice edge: Over ice, deep surface and elevated inversions were associated with alternating moist and dry layers in the lower troposphere; over water, multiple elevated inversions were associated with an elevated lower-tropospheric moist layer and dry regions near the surface and aloft. Possible physical processes important for the development of the observed features are discussed.

Handwritten: 11-11-87



Approved For	<input checked="" type="checkbox"/>
Excluded From	<input type="checkbox"/>
Classification	<input type="checkbox"/>
Declassify On	<input type="checkbox"/>
Authority	<input type="checkbox"/>
Comments	<input type="checkbox"/>
Signature	<input type="checkbox"/>
Date	<input type="checkbox"/>
Initials	<input type="checkbox"/>
Handwritten: A-1	

TABLE OF CONTENTS

I. INTRODUCTION	1
A. GENERAL	1
B. MARGINAL ICE ZONE EXPERIMENTS	1
C. PURPOSE AND SCOPE OF THESIS	4
II. ARCTIC MARINE BOUNDARY LAYER	5
A. GENERAL ATMOSPHERIC BOUNDARY LAYER FEATURES	5
B. MARCH-APRIL MIZ CLIMATOLOGY	6
1. Distinctive Features	6
2. Spring Climatology	9
3. Meteorological Conditions During MIZEX-87	11
III. DATA ACQUISITION AND PROCESSING	13
A. DATA ACQUISITION	13
1. Ship Configuration	13
a. Haakon Mosby	13
b. Polar Circle	13
c. Valdivia	13
2. Rawinsondes	14
B. DATA PROCESSING	15
IV. FLOW REGIME STUDIES	17
A. FLOW REGIME SYNOPTIC PATTERNS	17
B. BOUNDARY LAYER STRUCTURE	18
1. On-Ice Flow	18
2. Off-ice flow	32
3. Parallel Flow	38
V. SUMMARY AND RECOMMENDATIONS	50
A. SUMMARY	50
B. RECOMMENDATIONS	51

LIST OF REFERENCES	52
--------------------------	----

INITIAL DISTRIBUTION LIST	54
---------------------------------	----

LIST OF TABLES

Table 1. SUMMARY OF METEOROLOGICAL MEASUREMENTS	14
---	----

LIST OF FIGURES

Fig. 1.	OP-03 Severe weather operating goals.	2
Fig. 2.	MIZEX-87 operations area (MIZEX-87 Operations Plan).	3
Fig. 3.	The convective atmospheric boundary layer.	6
Fig. 4.	Climatological 700mb heights for April	7
Fig. 5.	Mean sea-level pressures for April	9
Fig. 6.	Climatological storm tracks	10
Fig. 7.	Time-series of meteorological parameters during MIZEX-87	12
Fig. 8.	Ship positions for 26 March 1987 with vector surface winds	19
Fig. 9.	Sea-level pressure analyses for off-ice flow	20
Fig. 10.	NOAA-10 AVHRR Channel 4 photo for 1658 UTC 26 March 1987.	21
Fig. 11.	Valdivia rawinsonde profiles for 26 March 1987	23
Fig. 12.	Polar Circle rawinsonde profiles for 26 March 1987	24
Fig. 13.	Haakon Mosby rawinsonde profiles for 26 March 1987	25
Fig. 14.	Cross-section for 12 UTC 26 March 1987	26
Fig. 15.	Cross-section for 18 UTC 26 March 1987	27
Fig. 16.	Cross-section for 12 UTC 27 March 1987	29
Fig. 17.	Ship positions for 27 March 1987, with vector surface winds	30
Fig. 18.	Time-section of Polar Circle soundings for 26, 27 March 1987	31
Fig. 19.	Sea-level pressure analysis for 12 UTC 4 April 1987.	33
Fig. 20.	NOAA-10 AVHRR photo for 1022 UTC 4 April 1987.	34
Fig. 21.	Ship positions for 4 April 1987, with vector surface winds	35
Fig. 22.	Time-section of Polar Circle radiosondes for 3, 4 April 1987	37
Fig. 23.	Polar Circle rawinsonde profiles for 4 April 1987	38
Fig. 24.	Time-section of Haakon Mosby radiosondes for 3, 4 April 1987	39
Fig. 25.	Haakon Mosby rawinsonde profiles for 4 April 1987	40
Fig. 26.	Sea-level analysis for 12 UTC 7 April 1987.	41
Fig. 27.	NOAA-9 AVHRR Channel 4 photo for 0533 UTC 7 April 1987.	42
Fig. 28.	Ship positions for 7 April 1987, with vector surface winds	44
Fig. 29.	Time-section of Polar Circle soundings for 7, 8 April 1987	45
Fig. 30.	Polar Circle rawinsonde profiles for 7 April 1987	46

Fig. 31. Time-section of Haakon Mosby soundings for 7-8 April 1987	47
Fig. 32. Haakon Mosby rawinsonde profiles for 7 April 1987	48

ACKNOWLEDGEMENTS

I would like to extend my sincere thanks to Professors K. L. Davidson, P. A. Durkee, and Mr. Peter Guest for their guidance, insight and support during the course of this research. Their assistance and attention to detail contributed to the success of this work. I would also like to thank Mr. Robert Fett and Mr. Ron Picard of the Naval Environmental Prediction Research Facility (NEPRF) for their comments and assistance with satellite imagery, and Dr. James Overland of the NOAA Pacific Marine Environmental Laboratory for his helpful discussion.

Finally, I would like to express my sincere appreciation to my wife, Betsy, for her untiring love, support and encouragement during the completion of this thesis and all my endeavors.

I. INTRODUCTION

A. GENERAL

The Arctic region has experienced greatly increased interest over the last two decades, due largely to the search for non-renewable resources (Westernlever, 1984). As energy resources, such as oil and gas, become increasingly difficult to find in less demanding locales, the difficulties of exploration and extraction in the Arctic become more acceptable. Research on the meteorology and oceanography of the region has occurred in response to petroleum industry needs (Merbs, 1988). Associated with increased national economic interest is the growing realization of the strategic importance of the region. The increased use of the Arctic as a deployment area for the strategic forces of the Soviet Union has forced the United States to enhance its operating capabilities in this vital region of the world. Research on the meteorology and oceanography of the region for United States Navy needs has been carried out for several years, funded by the Office of Naval Research, with the most recent series of experiments occurring in the east Greenland Sea and Fram Strait region (Johnson *et al.* 1984).

The Greenland Sea region represents an especially important area along the Arctic rim because it is the only deep water access to the Arctic Ocean. It therefore plays an important role in the deployment of naval forces should hostilities occur. An example of the emphasis placed on this area is the United States Navy's Arctic Cold Weather Surface Ship Plan developed by the Vice Chief of Naval Operations for Surface Warfare (OP-03). As shown in Fig. 1, the Navy intends to expand its operating limits northward to the marginal ice zone (MIZ) by the year 2010. In order to support the Navy's goals, as stated by OP-03, improvements in the ability to predict and avoid severe weather, and our knowledge of the region as a whole, are required.

B. MARGINAL ICE ZONE EXPERIMENTS

The east Greenland Sea marginal ice zone (MIZ) occurs where polar and temperate climatic systems interact to form a transition between ocean and pack ice regimes (Johannessen, 1987). As a geophysical boundary, the MIZ is unique in the complexity of the vertical and horizontal interactions that take place. Extensive seasonal variations in the ice edge boundary directly affect the heat and moisture available for exchange with the atmosphere, significantly impacting both the local atmospheric boundary layer

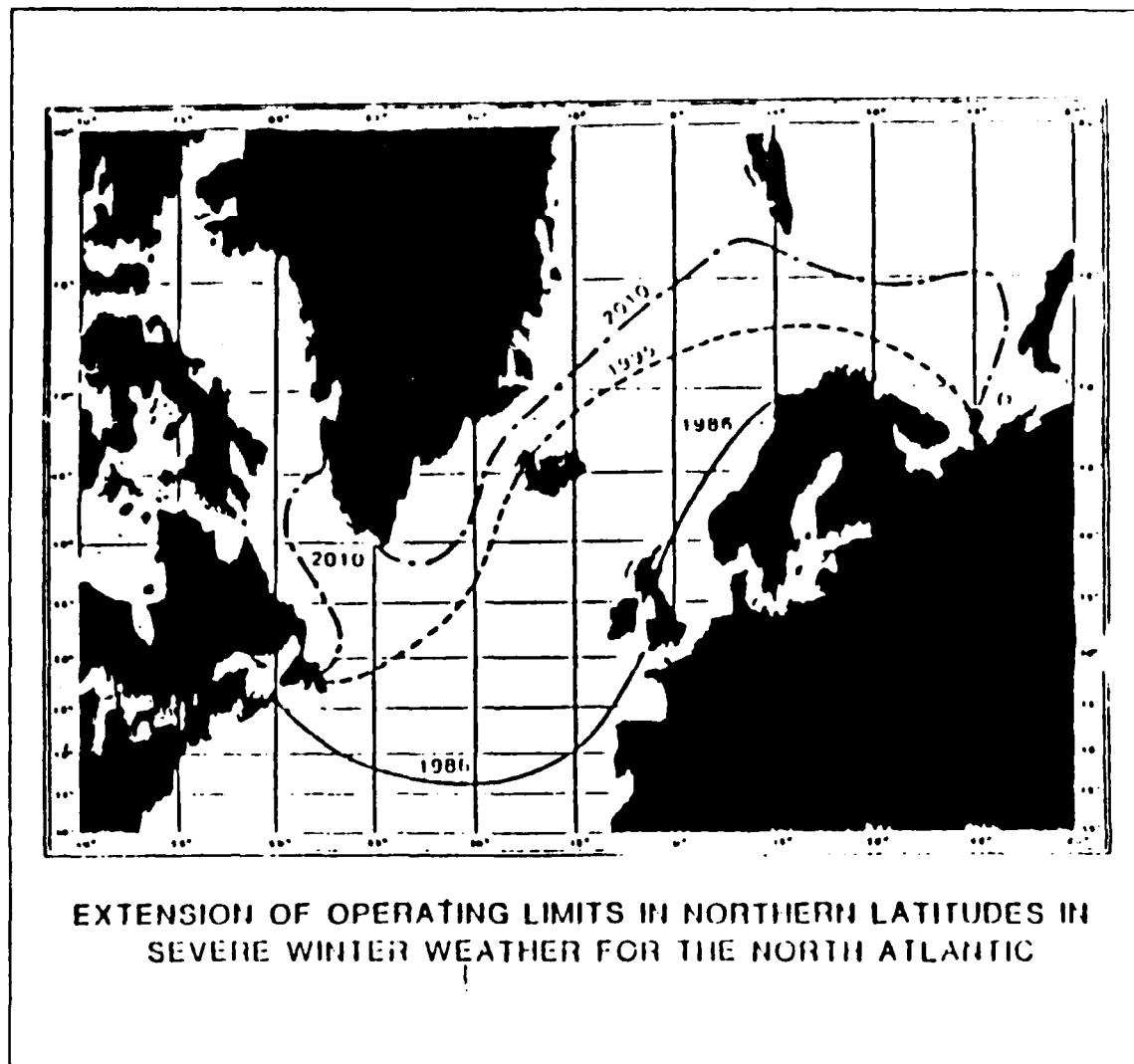


Fig. 1. OP-03 Severe weather operating goals.

(ABL) structure and the global climate (Johnson and Hawkins, 1987). In addition, the MIZ is a region of enhanced biological activity.

The Marginal Ice Zone EXperiment (MIZEX) series was developed in response to increased scientific, economic and strategic interest in the MIZ. The purpose of the MIZEX program is coordinated, multi-disciplinary studies of the physical and biological processes associated with a MIZ. The first two experiments of the series, MIZEX-83, conducted during June and July 1983, and MIZEX-84, conducted from May through

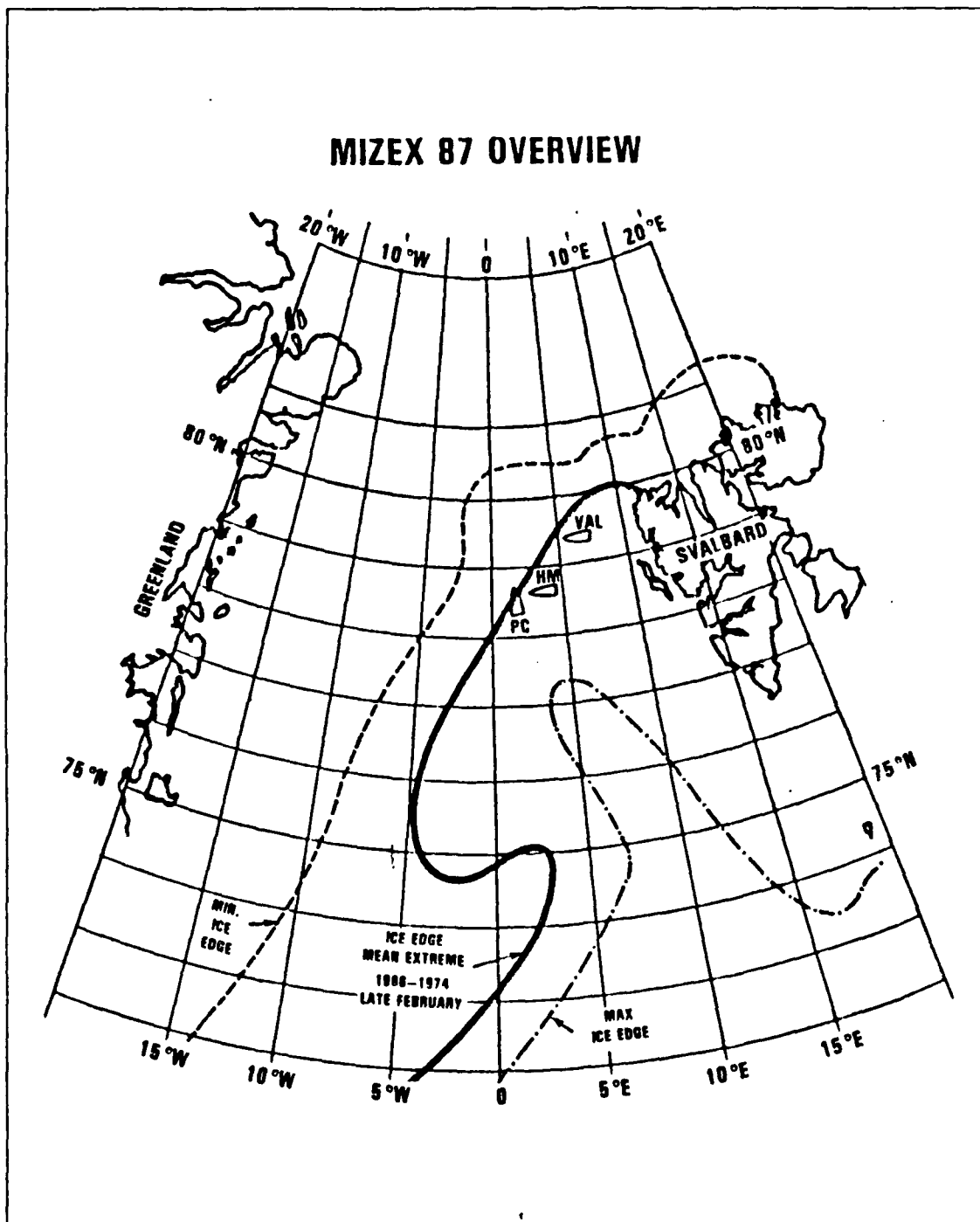


Fig. 2. MIZEX-87 operations area (MIZEX-87 Operations Plan).

July 1984, focused on processes and features of the Greenland Sea Fram Strait area during the summer regime.

Several investigations of the atmospheric boundary layer (ABL) processes unique to the MIZ were conducted with field observations taken during these first MIZEX experiments, together with model computations. The characteristics of the ABL and low-level flow observed during MIZEX-83 and MIZEX-84 are discussed in several recent papers (Kellner *et al*, 1987; Anderson, 1987; Fairall and Markson, 1987; Guest and Davidson, 1987; Guest *et al*, 1988; Overland, 1985). Results of a slab-symmetric model for the ABL together with field observations (Overland, *et al*, 1983) show the development of an inversion and other features over the Bering Sea MIZ during off-ice flow. More recent work by Overland (1988) and Kantha and Mellor (1988) describe more detailed multi-layer models of the ABL associated with the MIZ.

A late winter MIZEX was conducted from 20 March to 10 April 1987 in the Greenland Sea MIZ. This is referred to as MIZEX-87. The operations area for MIZEX-87, shown in Fig. 2, is the same region as in MIZEX-83 and MIZEX-84. MIZEX-87 is of special interest because data obtained represent one of the first data sets for the Greenland Sea MIZ during late winter conditions.

C. PURPOSE AND SCOPE OF THESIS

The purpose of this thesis is to examine boundary layer features and conditions during MIZEX-87 under three specific wind flow regimes with respect to the ice edge: on-ice flow, off-ice flow, and flow parallel to the ice edge. Structural features of the ABL are often associated with advection of air masses with respect to the ice edge, with rapid changes in the ABL accompanying shifts in wind direction. Sharp horizontal changes in heat, moisture and momentum fluxes associated with the ice edge cause rapid modification of the atmospheric boundary layer even in stable synoptic regimes, leading to unusual complexity in its vertical structure. Rawinsonde data from three ships during MIZEX-87 were used as input to a vertical cross-section program, allowing documentation of unique ABL features in the MIZ, and their temporal and spatial variability. The scope of this thesis is to present detailed physical descriptions of boundary layer features and changes resulting from shifts in the wind flow regime, and to discuss plausible physical explanations for the development of observed features. It is the intent of this thesis to provide an initial examination of a unique data set in the late winter Greenland Sea MIZ boundary layer, for each of the basic flow regimes.

II. ARCTIC MARINE BOUNDARY LAYER

A. GENERAL ATMOSPHERIC BOUNDARY LAYER FEATURES

The atmospheric boundary layer (ABL) is that portion of the atmosphere that is largely composed of air that has recently been in contact with the earth's surface, according to Stewart (1979). All momentum, moisture and heat exchanges between the surface and the atmosphere occur within this layer, so the boundary layer is clearly important to both the dynamic and thermodynamic structure of the atmosphere and surface. Typically over land, boundary layer depth may vary from tens to thousands of meters, while over the ocean a more constant depth of roughly 1 kilometer is recorded (Lenschow, 1986).

The ABL is a region of turbulent flow. Turbulence in the ABL is a function of surface roughness (parameterized by drag coefficient C_d), the vertical gradient of the near surface wind, and sensible and latent heat fluxes from the surface and atmosphere. Mechanical turbulence is produced by air flowing over a rough surface, transferring energy from the mean wind to turbulent eddies. This process is constantly at work to some degree in the ABL. Convective turbulence is produced by sensible and latent heat fluxes at the surface, or by latent heat flux aloft due to cloud formation, causing rising plumes of turbulent air. These turbulent plumes increase both the turbulent kinetic energy (TKE) and the mixing within the ABL. An increase in TKE usually results in an increase in ABL depth (Wyngaard, 1973).

The ABL can be described in terms of its density structure as unstable, stable, or neutral. An unstable ABL is produced by heating at the surface, leading to both convective and mechanical turbulence. A near surface wind shear zone called the surface layer transports wind momentum downward to the surface, and heat and moisture upward into a homogeneous layer constantly stirred by turbulence, called the mixed layer. This mixed layer is highly variable in depth, and comprises most of the ABL volume. The mixed layer is capped by a stably stratified region of vertically increasing temperature called an inversion, where turbulence is suppressed. These various layers are schematically represented in Fig. 3.

By contrast, a stable ABL is produced by cooling at the surface. This leads to development of an inversion near the surface and the suppression of convective turbulence. The remaining mechanical turbulence is able to mix only a shallow layer near the

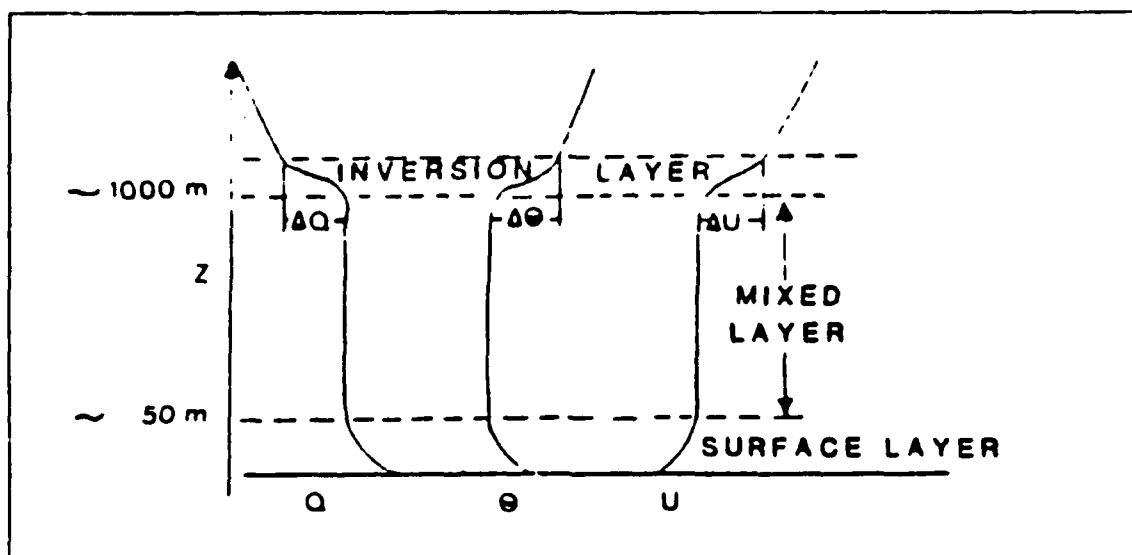


Fig. 3. The convective atmospheric boundary layer.: Mean vertical profiles of potential temperature (θ), wind speed (U), and specific humidity (q) are superimposed.

surface. This reduces both the upward mixing of heat and moisture, leading to sharper vertical gradients in these parameters, and the downward mixing of momentum, resulting in weaker surface winds than in the unstable case (Stewart, 1979).

The marine atmospheric boundary layer (MABL) differs from the ABL over land due to the influence of the ocean. The greater heat capacity of the ocean reduces the diurnal variations of surface heating, leading to a more constant depth for the MABL. The source of moisture at the ocean surface allows greater vertical gradients of moisture. Also, as air flows over the ocean for long distances, its properties move towards equilibrium with the surface, leading to near-neutral stability of the MABL. Small variations in sea-surface temperature, and therefore stability, can have significant effects on the structure of the MABL (Businger and Shaw, 1984).

B. MARCH/APRIL MIZ CLIMATOLOGY

1. Distinctive Features

Several unique features of the Arctic are important to the synoptic and local weather patterns of the region. Variations in these weather patterns force important modifications in the MABL through changes in the distributions of temperature, momentum, and moisture. These features are identified in Sater *et al* (1971) as unique

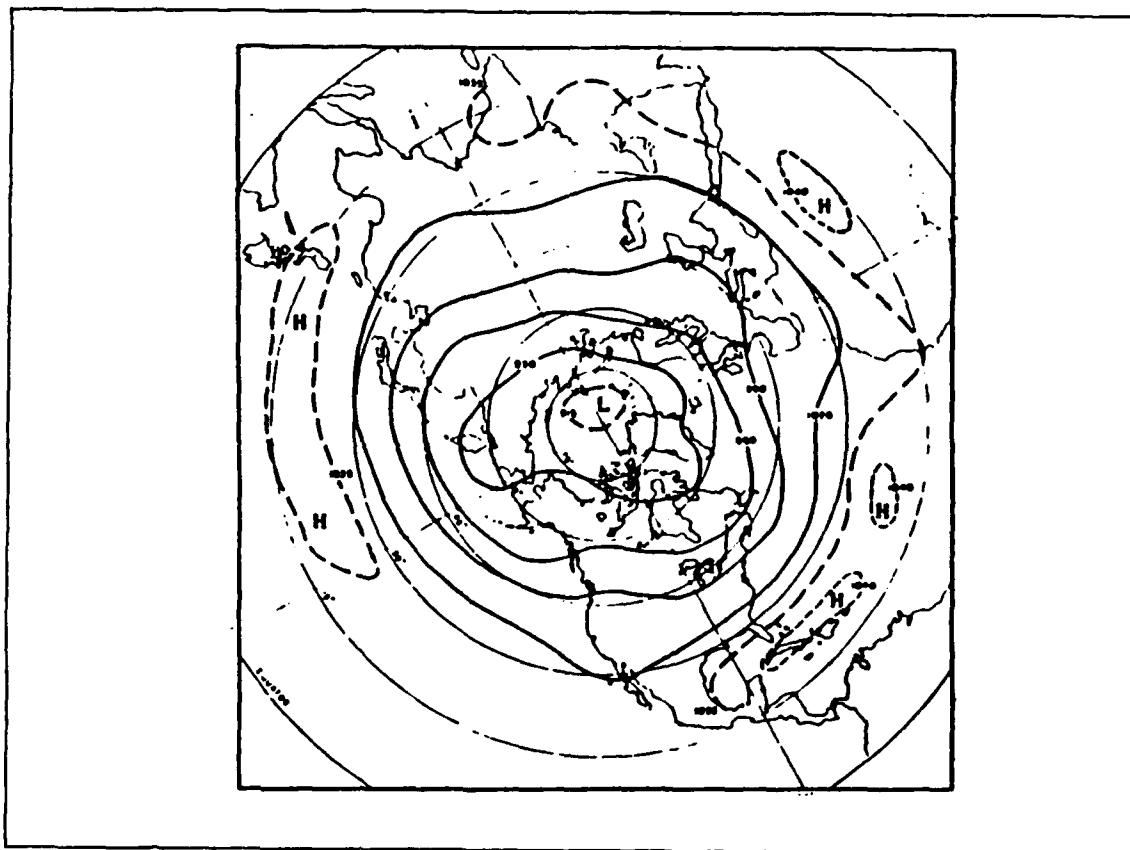


Fig. 4. Climatological 700mb heights for April: Sater *et al.* 1971.

daylight and darkness regimes and the circumpolar vortex, which are important for synoptic forcing, and surface ice cover and strong surface temperature inversions, important for local modification of the MABL. The combined importance of both synoptic and local forcing of the atmosphere distinguishes the Arctic regime.

Distinctive daylight and darkness regimes in high latitudes are a result of the earth's axial tilt. During winter, constant darkness contributes to a strong radiational heat loss at the earth's surface. In summer, total daylight reduces the net radiational loss at the surface. March and April mark the rapid transition from darkness to daylight regimes. Daylight increases from 9 hours in mid-March to 21 hours in mid-April, which encompasses MIZEX-87 (Schultz, 1987).

The circumpolar vortex, another unique feature, is a large scale cold core low pressure region approximately centered on the North Pole, and the belt of upper-level westerlies that surround the low at its outer edge (Petterssen *et al.*, 1956). The strength of this feature is usually associated with the packing of the 960 and 990dm isoheights

on the 700mb surface, as seen in Fig. 4. High latitude cyclones and anticyclones are embedded in and are steered by this flow, and changes in the strength and shape of the vortex can radically affect regional conditions (Sater *et al.*, 1971). During March and April, the vortex is in transition from its southernmost winter position to its northernmost summer position, with weakening of its associated pressure and temperature gradients.

The polar ice cap, covering the central Arctic and a large portion of the Greenland Sea, is a controlling factor in the climatology of the area. The high surface albedo properties of snow and ice, combined with low solar elevation angles, promote continuing cold surface temperatures over the ice pack. Cold temperatures greatly reduce the moisture capacity of air masses over ice compared to those over open ocean. Ice cover also insulates the atmosphere from the relatively warmer ocean below. The resulting moisture and temperature gradients near MIZ areas are strongly conducive to cyclogenesis and cloud formation. Therefore this factor is of great interest in discussions of weather patterns and boundary layer structure in and around the MIZ. During March the ice pack has achieved its maximum coverage before spring warming causes retreat of the ice edge. Fig. 2 indicates the large extent of the ice during this period.

Strong surface temperature inversions over the ice pack are a predominant feature of the Arctic atmosphere through the entire year. Arctic inversions are most often due to radiative cooling at the surface, creating stable ABL conditions, but elevated inversions may form due to advection or subsidence, typically extending above 850mb (Vowinckel and Orvig, 1970). This stable layer inhibits heat and moisture transfers across the inversion, creating a cold, moist layer near the surface and warmer, dry air above (Sater *et al.*, 1971). In ice free areas, the warm ocean surface causes elevated inversions due to positive heat flux and mixing, typical of unstable ABL conditions.

Another important feature specific to the MIZ is the rapidly changing drag coefficient (C_d) due to variable surface features. Pressure ridging, broken and jagged ice floes, and various types of newly formed ice such as grease ice or pancake ice contribute to much higher values of C_d in the MIZ than are measured in the central ice pack or over the open ocean (Guest and Davidson, 1987). This causes a drastic change in the formation of mechanical turbulence within the ABL over the short horizontal scales of the MIZ.

The combination of these unique features of the Arctic point out why ABL studies under various flow regimes along the ice edge are so important. Changes in the ABL structure, forced by flow along or across the MIZ and its variable surface

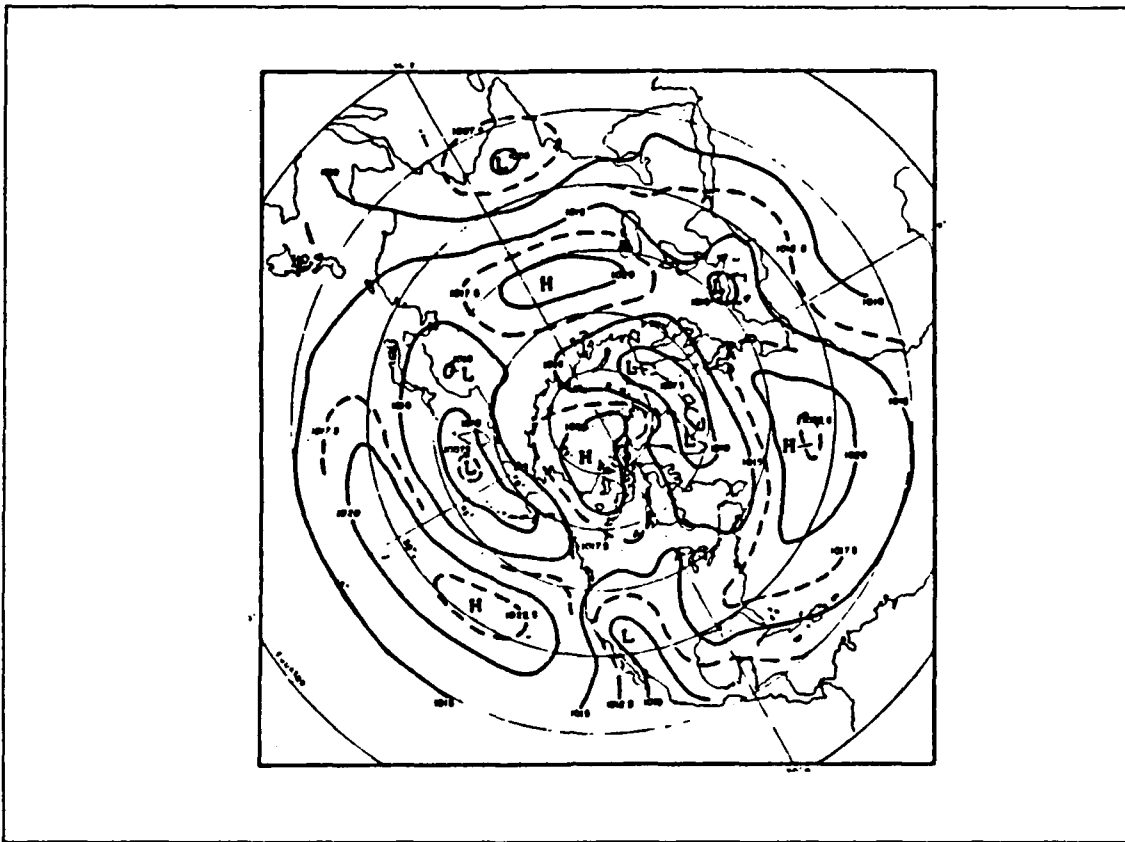


Fig. 5. Mean sea-level pressures for April: Sater *et al*, 1971.

conditions, result in changes in the transport of heat and moisture through the ABL to the upper atmosphere. Since the ability to forecast weather depends on a knowledge of these parameters, an understanding of changing ABL conditions is necessary for weather prediction in the region, and allows more accurate inputs for global prediction models. An understanding of the Arctic ABL has importance for ocean prediction as well. Downward transport of momentum from upper-level winds through the ABL to the surface drives ocean circulation and ice movement. Changes in ABL structure affect this downward momentum flux, and therefore affect future ice movements and current features.

2. Spring Climatology

The Greenland Sea MIZEX-87 experiment region is affected by several climatological synoptic-scale surface features. The 12-year climatological mean sea-level pressures for April are shown in Fig. 5. The spring MIZ surface synoptic pattern is characterized by a weak and variable surface high over northern Greenland and a belt

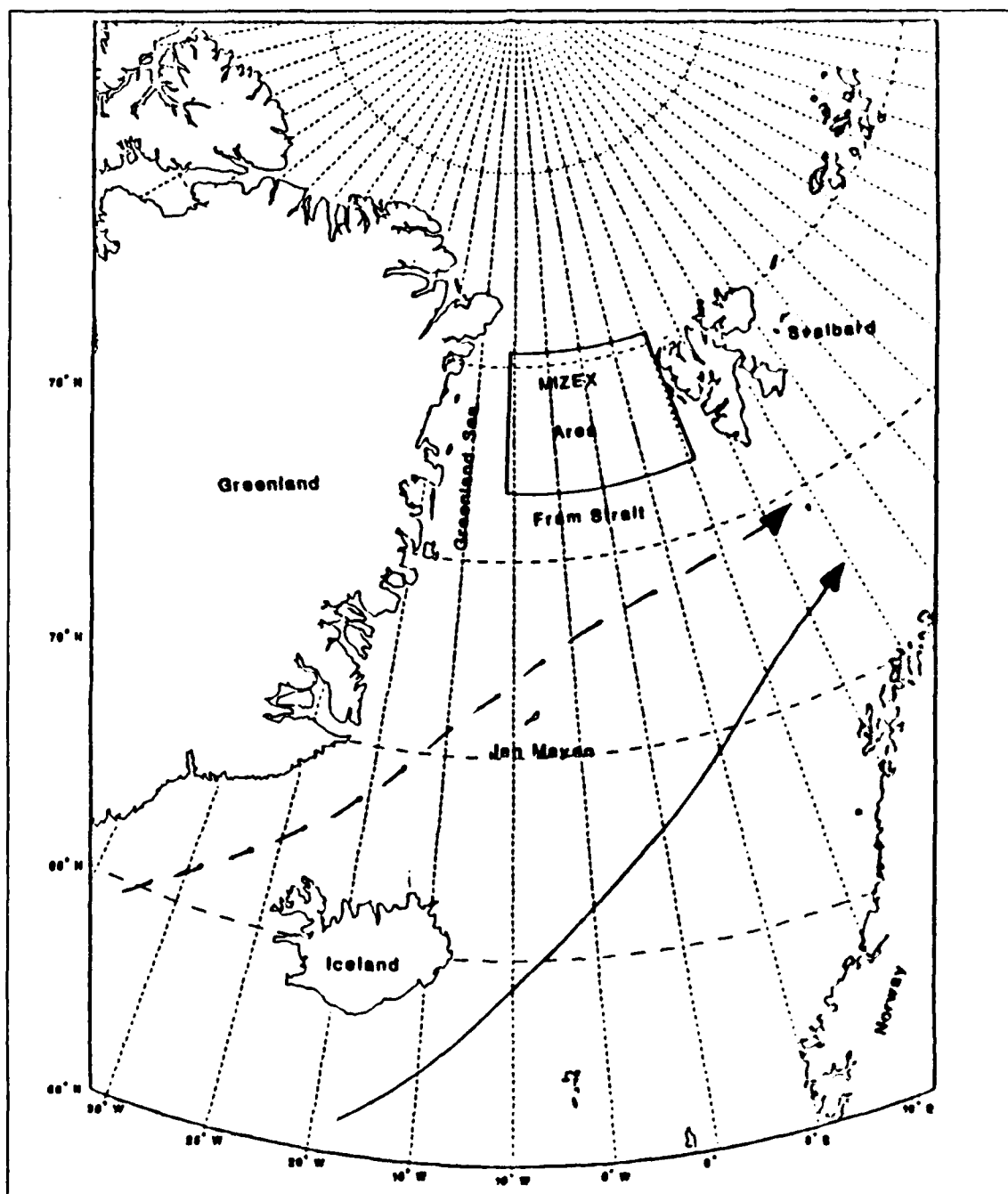


Fig. 6. Climatological storm tracks: Primary (solid) and secondary (dashed) storm tracks for April in relation to the MIZEX area, after Sater *et al.*

of low pressure extending from Iceland through the northern tip of Norway. This low pressure belt is strongly influenced by variations in the circumpolar vortex. Mean winds

in the MIZEX area are predominantly easterly due to the transitory cyclones to the south (Sater *et al.* 1971).

The climatological movements of cyclones in this area are related to the mean pressure gradients discussed above, and are clearly shown in Fig. 6. The primary storm track extends from the eastern coast of Iceland and continues to the northern tip of Norway. The secondary storm track follows the southeast coast of Greenland, then moves eastward passing just south of the Svalbard Islands, and into the decay region off northern Norway.

3. Meteorological Conditions During MIZEX-87

The synoptic and mesoscale meteorological features observed during MIZEX-87 were examined and grouped into five distinct periods by Schultz (1987). A time series of the major meteorological parameters observed during MIZEX-87 is shown in Fig. 7. Period one, from 20-23 March, saw a high pressure region centered over the Fram Strait. During period two, from 24-27 March, a mesoscale boundary layer front formed just west of the Svalbard Islands and propagated westward across the Fram Strait. The high pressure system weakened during this period causing surface pressures to fall. The third period was from 28-31 March, when the MIZEX area was influenced by a small scale low that stagnated and began to fill. In period four, from 1-3 April, the MIZEX area was again under the influence of a high pressure system. A synoptic-scale low passed to the south during this period. During the fifth and final period, from 4-10 April, the MIZEX region was influenced by two synoptic-scale lows. The first low moved slowly through the area along the secondary storm track, as seen in Fig. 6, and stalled SW of the Svalbard Islands on 5 April. A second low pressure system overtook and merged with the first low on 8 April, creating a larger, more intense low with significant influence on the region. Specific wind regimes during these synoptic periods will be selected for detailed study of the vertical boundary layer structure.

Groters (1988) and Schultz (1987), on examination of observed fields, concluded that during MIZEX-87 synoptic features were consistent with the climatology of the MIZEX region discussed earlier. The region was dominated by high pressure except during movement of synoptic-scale lows and the boundary layer front. Winds tended to be more northerly during MIZEX-87, contrary to the climatological easterly winds described by Sater *et al.* (1971). This indicates reduced influence or a lower frequency of synoptic-scale lows during this period.

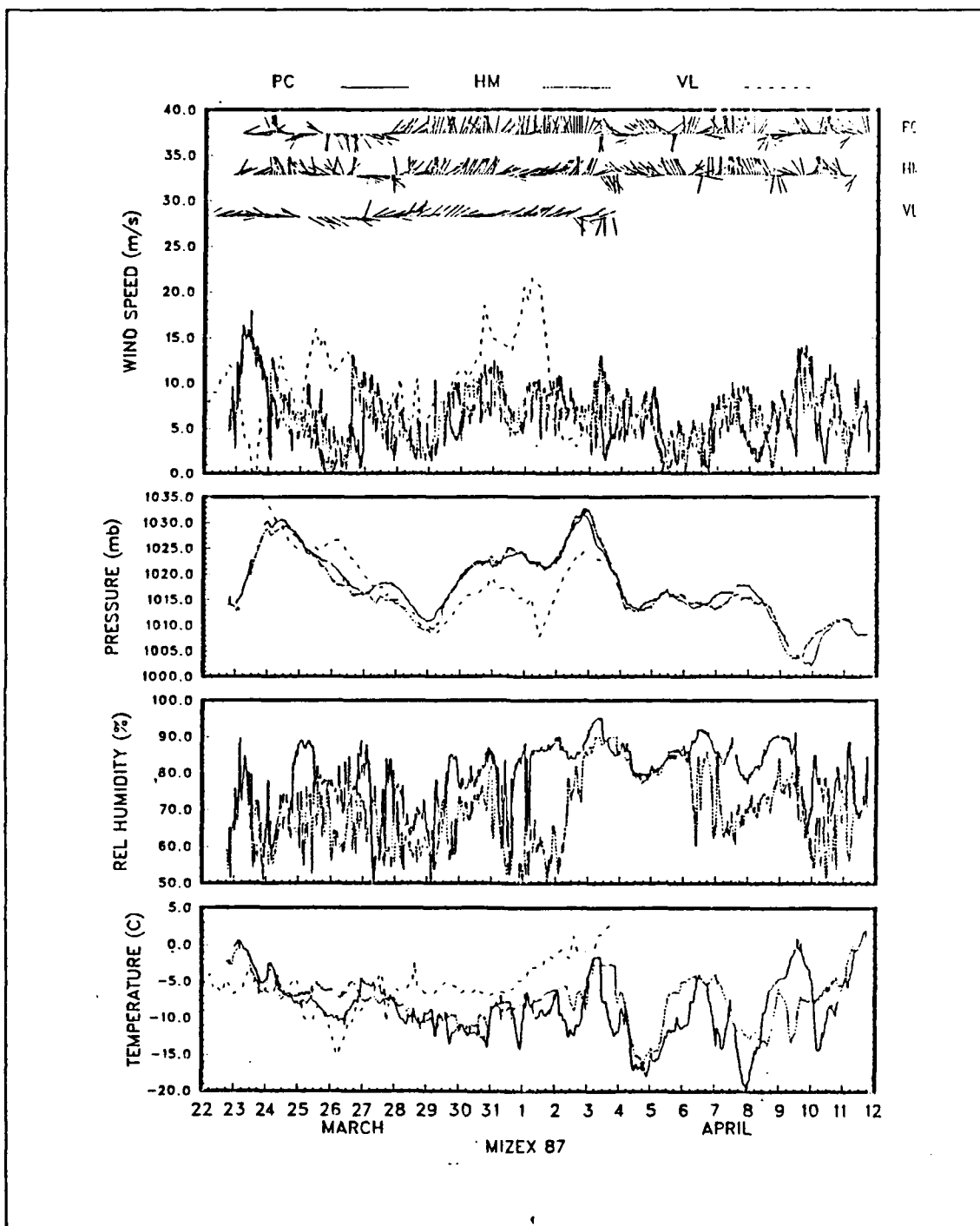


Fig. 7. Time-series of meteorological parameters during MIZEX-87 (Guest and Davidson, 1988).

III. DATA ACQUISITION AND PROCESSING

A. DATA ACQUISITION

Descriptions of the vertical boundary layer structure during MIZEX-87 were obtained from rawinsondes and surface layer measurements made from three surface ships operating in and around the MIZ. The research vessels Haakon Mosby, Polar Circle, and Valdivia launched radiosondes every six hours, made visual surface observations every three hours, and continuously recorded various meteorological data using ship mounted instruments. A list of the instruments and observed meteorological parameters on all ships appears in Table 1.

1. Ship Configuration

a. Haakon Mosby

The Haakon Mosby collected data in the MIZ from 23 March through 11 April 1987. Surface data, including wind speed and direction, pressure, relative humidity and temperature were collected using a meteorological instrument station mounted 18 m above the water line. Wind speeds were measured using propeller and cup anemometers. Wind direction was determined by magnetic compass, providing accuracy within five degrees of true direction. Pressure was recorded using automatic pressure sensors.

The above data were sampled continuously and results presented in this thesis represent ten-minute averages of these data. Guest and Davidson (1988) discuss in detail the various error sources for these meteorological instrument packages.

b. Polar Circle

The Polar Circle recorded MIZ data from 23 March to 12 April 1987. The same parameters were measured on the Polar Circle as on the Haakon Mosby, and were obtained using the same basic instrument package mounted 16 m above the water line. The only exception is that a sonic anemometer was used instead of the cup anemometer. Wind direction errors were much larger than for the Haakon Mosby due to extreme magnetic deviations introduced by the ship's hull. Therefore, accuracy for wind direction is within 20° (Guest and Davidson, 1988).

c. Valdivia

The Valdivia collected data from 19 March through 3 April 1987. The Valdivia measured the same parameters as discussed for the other ships, except without

Table 1. SUMMARY OF METEOROLOGICAL MEASUREMENTS

MEASUREMENT	INSTRUMENT	SHIP LOCATION	SAMPLE INTERVAL
Vector Wind Temperature Humidity	Propeller Anemometer Thermuster Hygrometer	PRC HKM VAL (Bow Mast)	10 Minute
Turbulent Vector Wind	Sonic Anemometer	PRC (Bow Mast)	10 Minute
Turbulent Wind Speed	Hot Film Miniature Cups	PRC HKM (Bow Mast)	10 Minute
Temperature Humidity Vector Wind	Rawinsonde	PRC HKM VAL	4 per Day
Sensible Wx Sea State	Human Observer	PRC HKM VAL (Bridge)	24 per Day
Incoming LW and SW Radiation	Pyranometer Pyrehelimeter	HKM (Upper Deck)	10 Minute
Boundary Layer Structure	Acou tic Sounder	HKM (Upper Deck)	10 Minute
Barometric Pressure	Barometer	PRC HKM VAL	10 Minute
(PRC = Polar Circle, HKM = Haakon Mosby, VAL = Valdivia)			

any relative humidity measurement. Due to timing errors in the recording equipment, the only available data were those recorded during surface observations which occurred every three hours. Accuracies are similar to those discussed for the Haakon Mosby.

2. Rawinsondes

Because of the importance of rawinsonde data to this study, a detailed discussion of the characteristics of the rawinsondes used during MIZEX-87 is included for clarity. A total of 169 successful launches were made during MIZEX-87: 66,48, and 55 each for the Polar Circle, Valdivia, and Haakon Mosby respectively. The Polar Circle and Valdivia used rawinsondes and a receiving station manufactured by the VIZ Corporation to obtain vertical profiles of atmospheric parameters. The VIZ-Beukers

W-8000 RP+ Microsonde system was the receiving system used by these two ships. The receiving station and rawinsondes allowed measurements of wind speed and direction, as well as pressure, temperature, relative humidity, and altitude. These radiosondes allow a sampling interval of every 10 seconds for a period of 50 minutes, providing a maximum of 300 vertical data points per launch. The wind speed and direction were measured using an Omega tracking system within the radiosonde. Air temperatures measured with this system were accurate to 0.2° C, with dewpoint temperatures accurate to 1.0° C. Altitudes were accurate to within 30 m. Wind speeds were accurate to 1.0 m s except in regions of strong wind shear, where wind speeds were within 2.0 m s (Guest and Davidson, 1988).

The Haakon Mosby used a RS-80 Microcora Upper Air Sounding system, manufactured by the Vaisala Corporation. The Vaisala sonde measured identical properties as the VIZ sonde, also using an Omega tracking system for wind direction and speed.

The vertical gradient of moisture is an important parameter in this discussion of boundary layer structure. Willis (1987) described a possible error in 37% of the radiosonde profiles used in her study of refractivity during MIZEX-84. In the suspect profiles, the dewpoint temperature equaled the air temperature just below the inversion, indicating saturation. At the inversion base, dewpoint normally decreases with height. The profiles examined by Willis did not follow this pattern. The dewpoint was observed to remain saturated through the inversion and decrease sharply at a variable distance above the inversion. Willis suggested an instrument error in these cases due to possible frost formation on the humidity sensor, and presented a correction method to reduce errors in the soundings. Groters (1988) examined MIZEX-87 radiosonde profiles for similar features in his study of refractive conditions, and found that the suspect profiles occurred in only 13 of 169 launches. While Groters also considered potential instrument errors in the suspect profiles, he determined that the dewpoint problem was not extensive enough to warrant use of the correction scheme suggested by Willis.

B. DATA PROCESSING

Rawinsonde data sets serve as the primary source of data for this study. Initial processing of the data included sorting, reformatting, and checking for errors in individual radiosonde data sets. Data display was achieved by a Fortran cross-section algorithm developed by the Department of Meteorology, Naval Postgraduate School.

The cross-section algorithm was modified to plot multiple radiosonde launches from the surface to 700mb. Data was processed to show both potential temperature (K) and specific humidity (g kg) as continuous lines, along with wind barbs every 10mb at each station. Specific humidity was computed based on vapor pressure calculations after Buck (1981). After potential temperature and specific humidity values were computed for each station in the cross-section, station data were projected onto a 50x50 plotting grid by linear interpolation routines. Contours of the gridded data were then computed using a smoothed rational spline interpolation method that allows curves to turn back on themselves. In practice, these data projection and interpolation methods created excellent cross-sections. However, with some data sets, the routines created bulls-eye features around isolated data points or plotted unusual features in data void regions. These unusual features were easily allowed for in analysis of the various cross-sections examined.

Spatial cross-sections were prepared when the Polar Circle, Haakon Mosby, and Valdivia were in optimum positions. In other cases, time-sections for individual ships were plotted.

IV. FLOW REGIME STUDIES

Observed data on the structure of the planetary boundary layer during MIZEX-87 were examined with respect to time and space variations in the inversion height, vector wind, temperature, and specific humidity that resulted from changes in wind flow regimes. Three specific flow regimes were chosen for study: a) On-ice flow, which was associated with easterly surface winds from the Fram Strait onto the MIZ and ice pack; b) Off-ice flow, which was associated with westerly surface winds from the ice pack and MIZ region towards the open ocean; and c) Parallel flow, associated with northeasterly winds flowing parallel to the ice edge, with the ice to the right of the wind.

No significant periods of parallel flow with the ice to the left of the wind occurred during MIZEX-87, therefore this case was not examined. Synoptic-scale forcing for this type of flow regime would typically involve high pressures to the southeast of the MIZ and low pressures to the west-northwest, a situation not favored during the spring period in this area.

A. FLOW REGIME SYNOPTIC PATTERNS

An on-ice flow regime occurred from 00 UTC 26 March to 00 UTC 28 March 1987. On-ice flow developed sequentially from east to west across the Fram Strait, due to movement of a boundary layer front that had developed about 100 km west of the Svalbard Islands. The boundary layer front is a common arctic feature observed to form in association with the ice edge. The fronts are observed to develop at the boundary between the cold dry air of the central ice pack and the warmer moist air over open water (Shapiro and Fedor, 1986). As a result of winds shifting to easterlies on 25 March, the boundary layer front moved rapidly across the Fram Strait and into the MIZEX area, stalled and dissipated. Although sea-level pressures dropped steadily from 1035mb to 1017mb during the period, an upper-level high persisted over the area.

An off-ice flow regime occurred from 18 UTC 3 April to 06 UTC 5 April 1987. Synoptic forcing for this regime was associated with the formation and movement of a synoptic-scale low south of the MIZEX area. This low formed rapidly about 100 km east of Greenland at 06 UTC 3 April, and moved along the secondary storm track presented in Fig. 6. The low stalled about 100 km southwest of the Svalbard Islands at 12 UTC 5 April.

A parallel flow regime occurred from 18 UTC 6 April to 06 UTC 8 April 1987. Synoptic forcing during this time period was associated with a second synoptic low forming at 06 UTC 4 April 100 km east of Greenland, similar to the low one day before. This second low also moved up the secondary storm track, and merged with the first low southwest of Svalbard on 8 April. The positions of these two lows with respect to the Greenland high caused parallel (southwest) flow through the MIZEN area.

B. BOUNDARY LAYER STRUCTURE

1. On-Ice Flow

Just prior to the beginning of the on-ice flow regime, the Polar Circle and Haakon Mosby transited from Tromsø, Norway to begin experiment operations. The Valdivia had been on station for several days near 78° N 0° E, her northern-most position during the experiment, and was underway, moving southward parallel to the Svalbard coast then southwest towards the north-south portion of the MIZ, west of the Fram Strait. The relative positions of the three ships, shown with vector surface winds in Fig. 8, provided a linear arrangement useful for spatial cross-section analysis of the radiosonde data. This linear arrangement tends NW-SE on 26 March, and rotates to nearly N-S by 28 March.

The sea-level pressure analyses for 00 UTC 26 March and 00 UTC 27 March are shown in Fig. 9. From 00 UTC 24 March to 00 UTC 25 March 1987, a boundary layer front was observed to form 100 km west of the Svalbard Islands, in association with an inverted trough that had developed over the Fram Strait. Decay of the trough caused easterly flow across the strait, resulting in an outbreak of Arctic air and advection of the front advected rapidly westward, reaching the MIZ by 00 UTC 27 March. Movement of this front across the Fram Strait is important because it precedes the shift in winds to on-ice (easterly). Another reason to document the movement of this front in this case is that it illustrates the rapid modification of a polar air mass due to the open waters of the Fram Strait. A NOAA-10 Channel 4 ($10.5 - 11.5 \mu\text{m}$) satellite photo presented in Fig. 10, shows the position of the front during its movement across the strait. Frontal passage first occurred at the Valdivia between 03 UTC and 06 UTC on 25 March. Passage of the front was marked by winds veering to southeasterly and increasing to 15 m/s , cloudiness increasing from 3/8 stratocumulus to 8/8 stratus, a sharp drop in temperature from -4.5°C to -10.5°C , and snow showers. Similar weather features were observed at the Haakon Mosby and the Polar Circle during frontal passage at 14 UTC 26 March and 23 UTC 26 March, respectively.

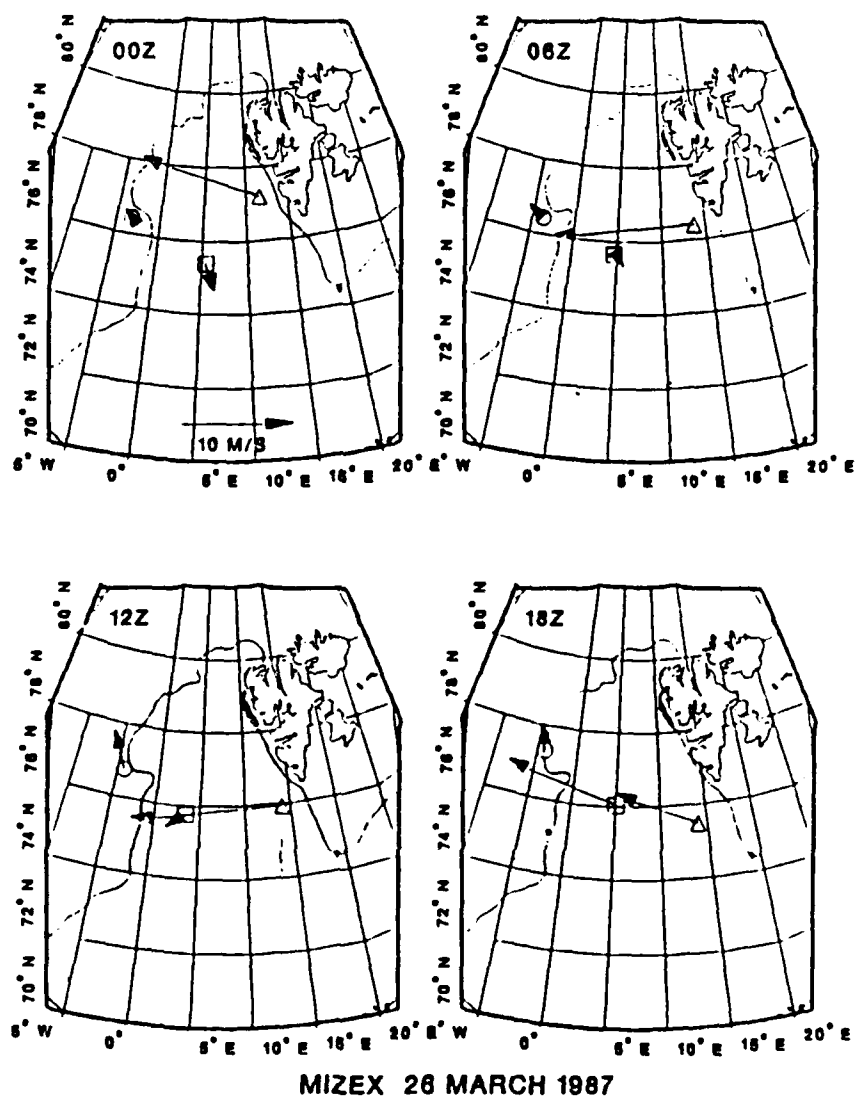


Fig. 8. Ship positions for 26 March 1987 with vector surface winds: Vector length is proportional to windspeed (scale in 00 UTC). Polar Circle = \circ , Haakon Mosby = \diamond , Valdivia = ∇ .

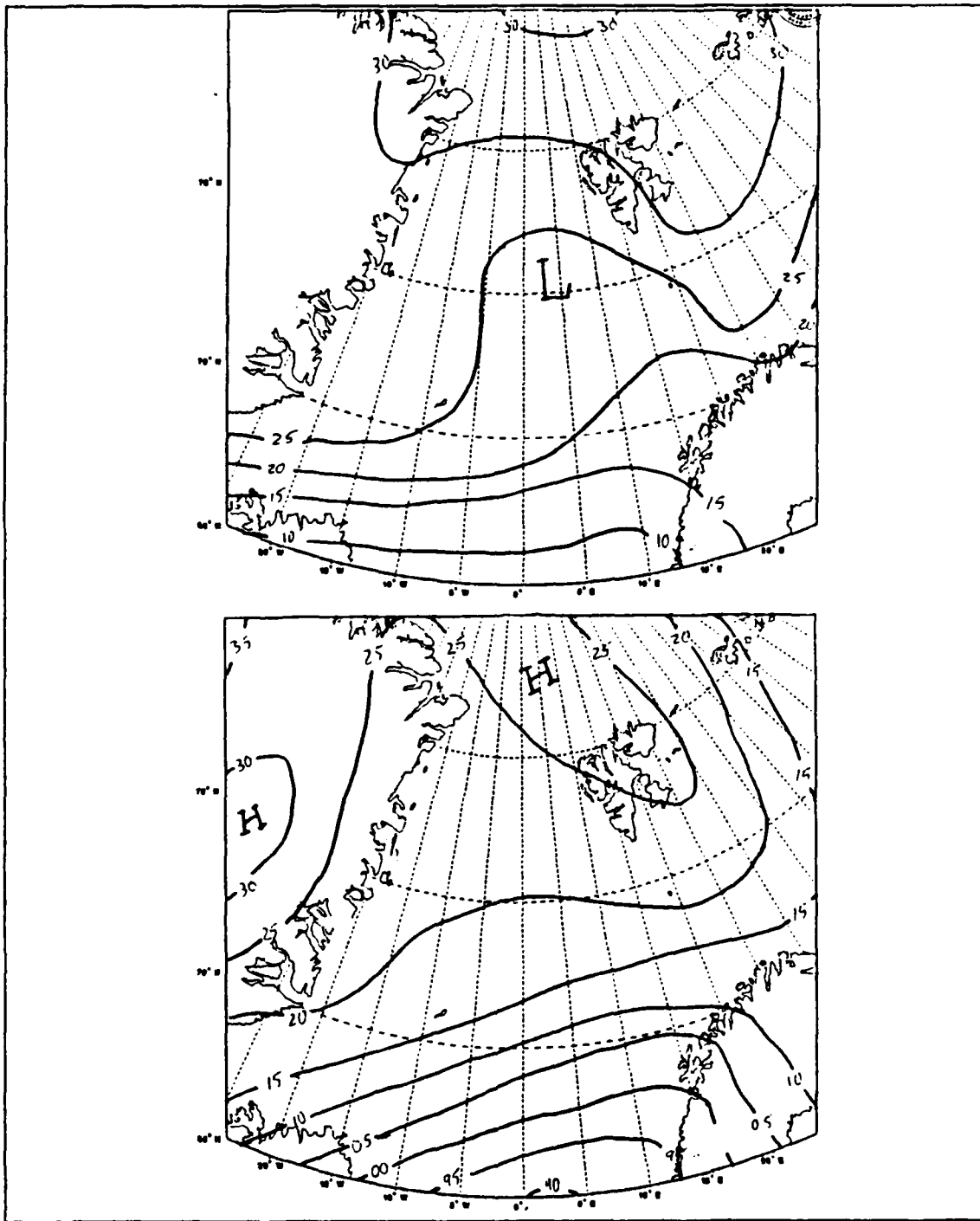


Fig. 9. Sea-level pressure analyses for off-ice flow: 00 UTC 26 March 1987 (top).
00 UTC 27 March 1987 (bottom).



Fig. 10. NOAA-10 AVHRR Channel 4 photo for 1658 UTC 26 March 1987.

Rawinsonde profiles observed at the Polar Circle, Haakon Mosby, and Valdivia are presented in Fig. 11, Fig. 12, and Fig. 13, respectively. All rawinsonde profiles shown in this thesis have the following key. The bold solid line is potential temperature (θ). The dashed line is potential dewpoint temperature (θ_d). Both of these use the bottom scale in $^{\circ}\text{C}$. The light solid line is specific humidity using the top scale in g kg.

Examination of the rawinsondes for the various ships point out major changes in the structure of the boundary layer due to passage of the front and subsequent on-ice flow. Valdivia profiles (Fig. 11) reveal a strong inversion between 800 and 900mb prior to frontal passage. Polar Circle radiosonde profiles (Fig. 12) and Haakon Mosby profiles (Fig. 13) also show the presence of strong inversions between 500 and 1000mb. The approach and passage of the boundary layer front causes rapid rising and destruction of these low-level inversions and establishment of a deep mixed layer. Winds veer to the southeast and strengthen as the front successively passes each ship, establishing an on-ice flow regime across the entire Fram Strait region by 00 UTC 27 March.

A spatial cross-section roughly perpendicular to the front at 12 UTC 26 March is shown in Fig. 14. All cross-sections and time-sections presented in this thesis have the following key. Solid lines indicate θ in K. Dashed lines indicate specific humidity in g kg. Winds are reported in m/s approximately every 10mb, and with speeds indicated by barbs (full barb = 5 m/s, half barb = 2.5 m/s).

The cross-section at 12 UTC reveals structural features of the boundary layer during frontal passage. At 12 UTC the front is well past the Valdivia at the eastern end of the cross-section, but has not completely moved past the Haakon Mosby, which recorded passage at 14 UTC. Easterly (on-ice) winds have been established at both the Valdivia and the Haakon Mosby.

The isentropes in the 12 UTC cross-section exhibit very strong tilting from west to east across the Fram Strait. This is due to the cold air outbreak from the Svalbard ice-pack moving west rapidly enough to maintain its polar characteristics in spite of the increased heat and moisture flux over the open water. The relatively warm air aloft over the western end of the cross-section is indicative of subsidence from the upper-level high. The Valdivia sounding, at the eastern (right) end of the cross-section, has evenly spaced isentropes throughout the vertical, with moderate gradients, indicating neutral stability. A weak inversion at 930mb (600m) appears to indicate that increased heat flux over the ocean is beginning to modify the polar air mass, and establish a mixed layer over the eastern Fram Strait. A strong moisture gradient not coincident with the weak inversion is noted at 850mb (1200m), with extremely cold dry air above. This marks the

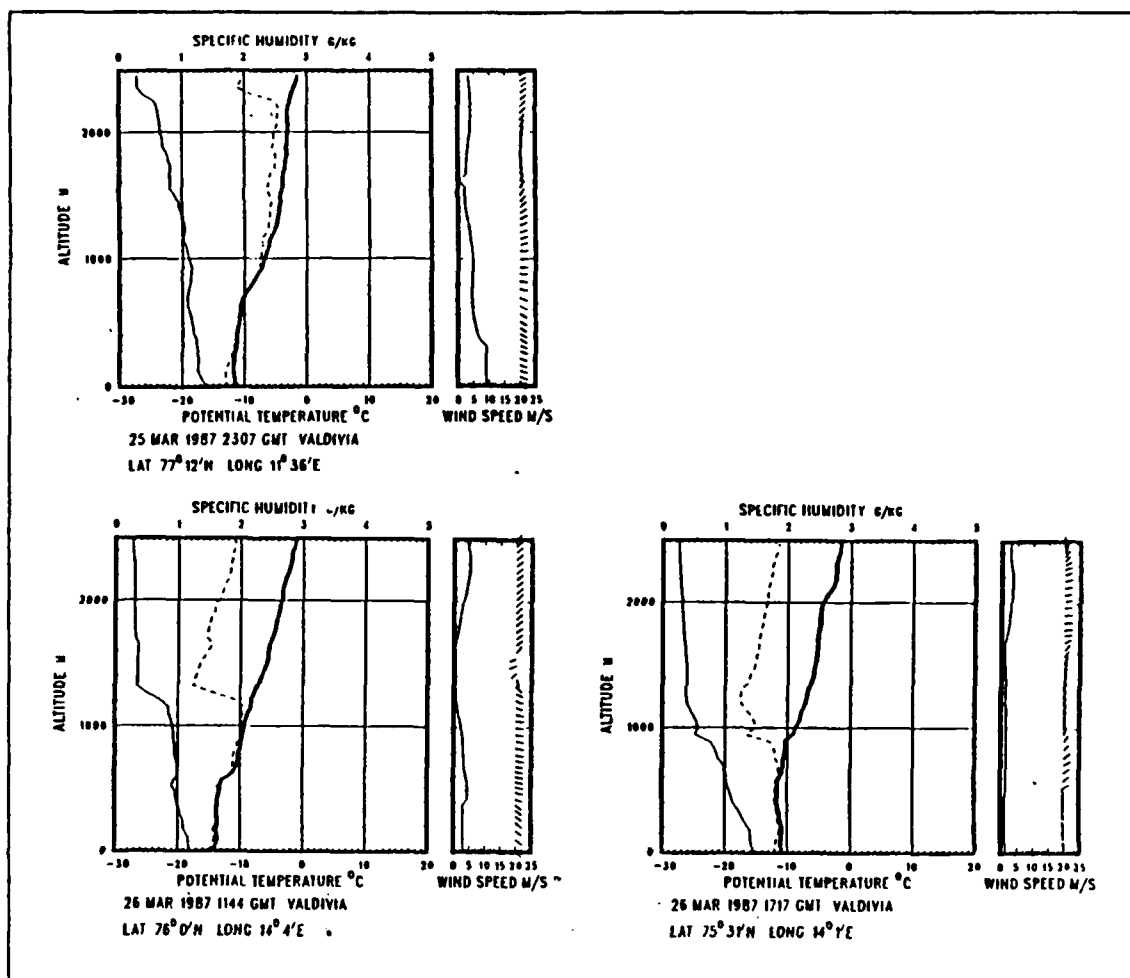


Fig. 11. Valdivia rawinsonde profiles for 26 March 1987: Bold solid line is θ . Dashed line is θ_d . Light solid line is q

unmodified polar air mass from the Svalbard ice pack. Winds remain easterly throughout the vertical, with a small reversal at 850mb coincident with the moisture gradient. This wind shift seems to mark the depth of the boundary layer at this point.

The profile from the Haakon Mosby, over the central Fram Strait, shows a dip in potential temperature between 900 and 1000mb, perhaps associated with frontal passage, and slight packing of the isentropes near the surface. Above 900mb, isentropes are again evenly spaced indicating neutral stability with no inversions noted. A strong moisture gradient occurs at 850mb (1500m) with extremely dry air above. This is again associated with a wind shift aloft, marking the boundary layer, and appears to extend

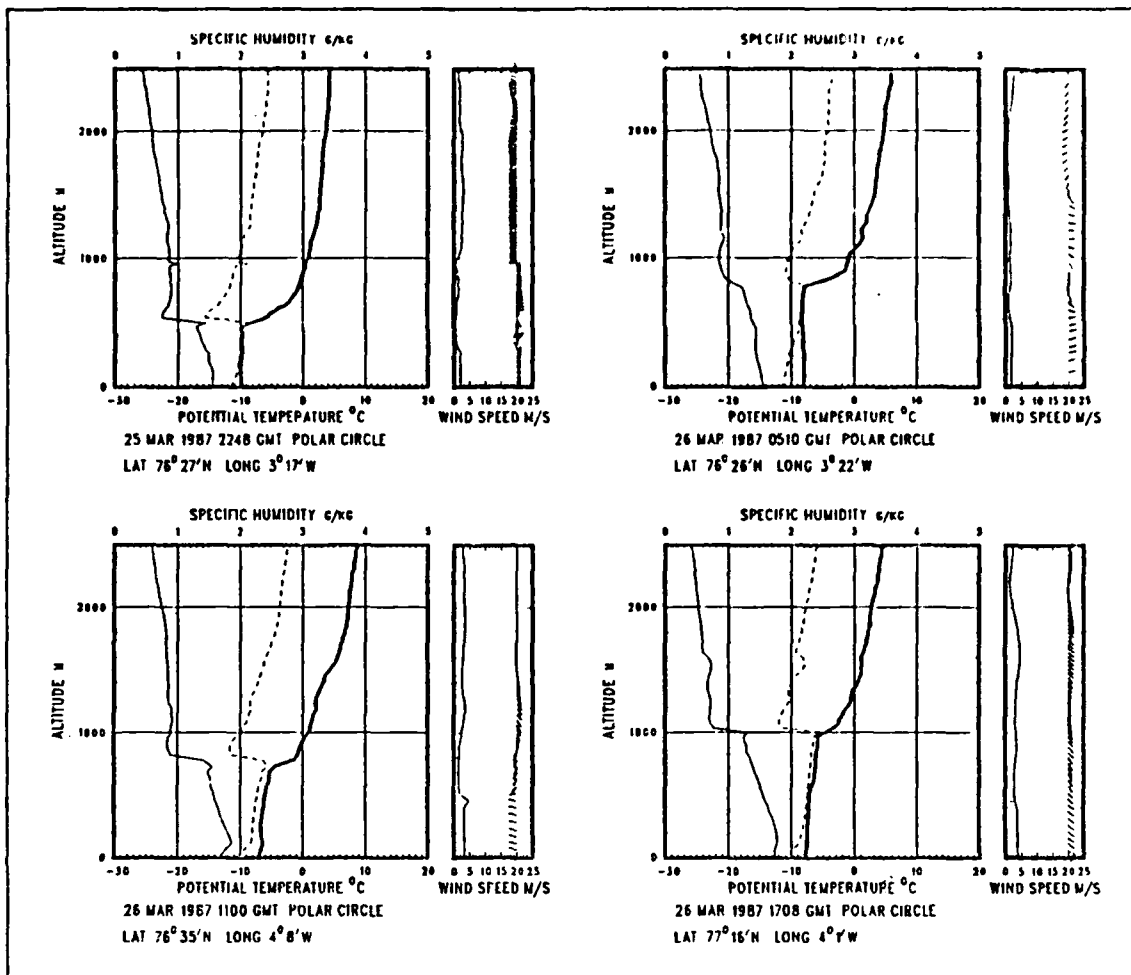


Fig. 12. Polar Circle rawinsonde profiles for 26 March 1987: Parameters as in Fig. 11

completely across the Fram Strait. Another interesting feature of the wind profile is the that the wind maxima associated with frontal passage appears between 930mb and 860mb, but has not penetrated to the surface.

The Polar Circle, at the western end of the section, has not yet recorded frontal passage and off-ice flow exists, although inversion heights at the Polar Circle have been rising steadily over the last 24 hours, as can be seen in the rawinsonde profiles shown in Fig. 13. At lower levels, a layer well mixed in temperature and moisture extends from the surface to 900mb (1000mb) where it is capped by a strong inversion coincident with a moisture gradient. This very moist well-mixed layer appears to extend eastward

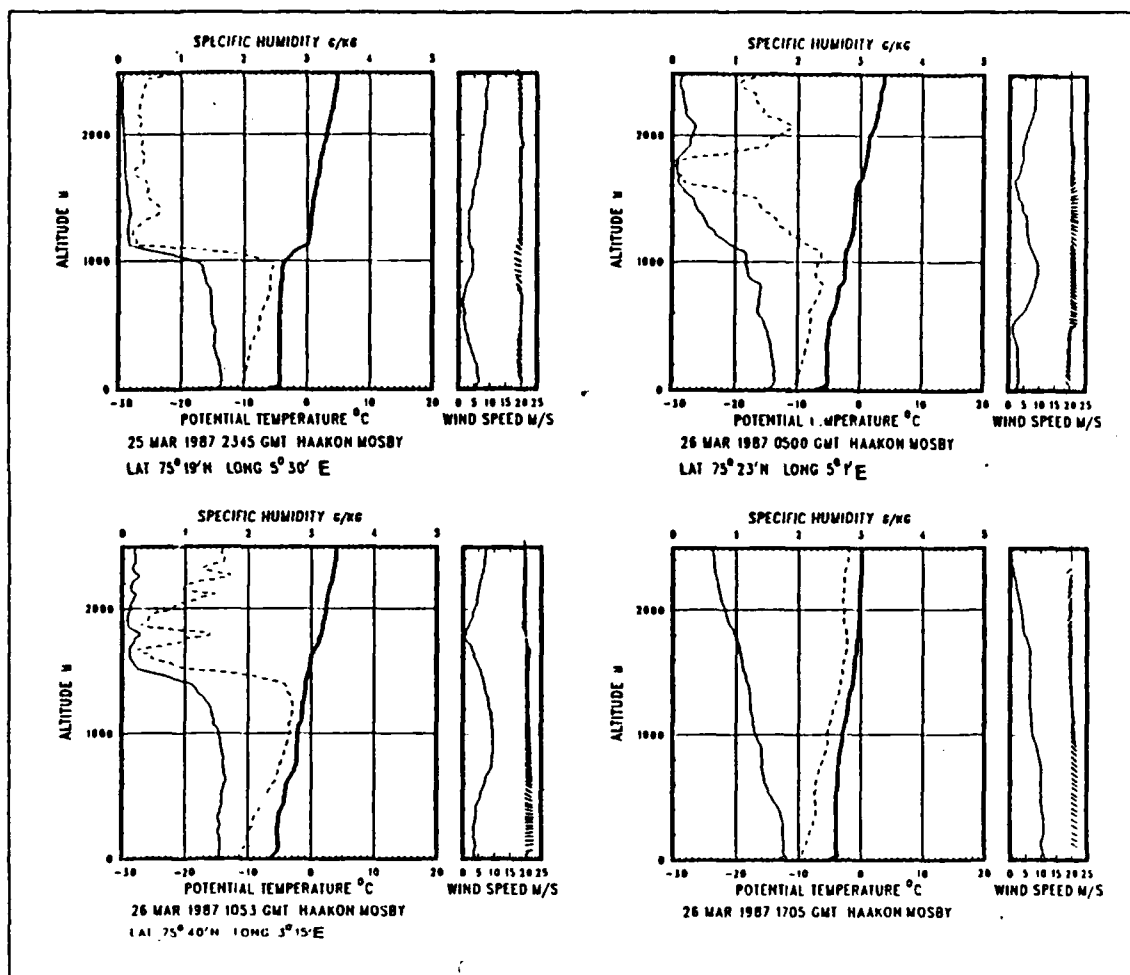


Fig. 13. Haakon Mosby rawinsonde profiles for 26 March 1987: Parameters as in Fig. 11

beyond the capping inversion nearly to the front itself. Above the inversion, moderate gradients in temperature and moisture extend to 700mb. A wind shift from westerly to southerly occurs at the inversion.

The front continues to be advected westward during 26 March. Fig. 15 presents a cross-section observed at 18 UTC 26 March, six hours later. By this time the boundary layer front has passed the Haakon Mosby, and has approached the Polar Circle's position at the MIZ, with easterly surface winds recorded at all three ships. The inversion previously noted at the Polar Circle has risen from 900mb to 860mb and weakened.

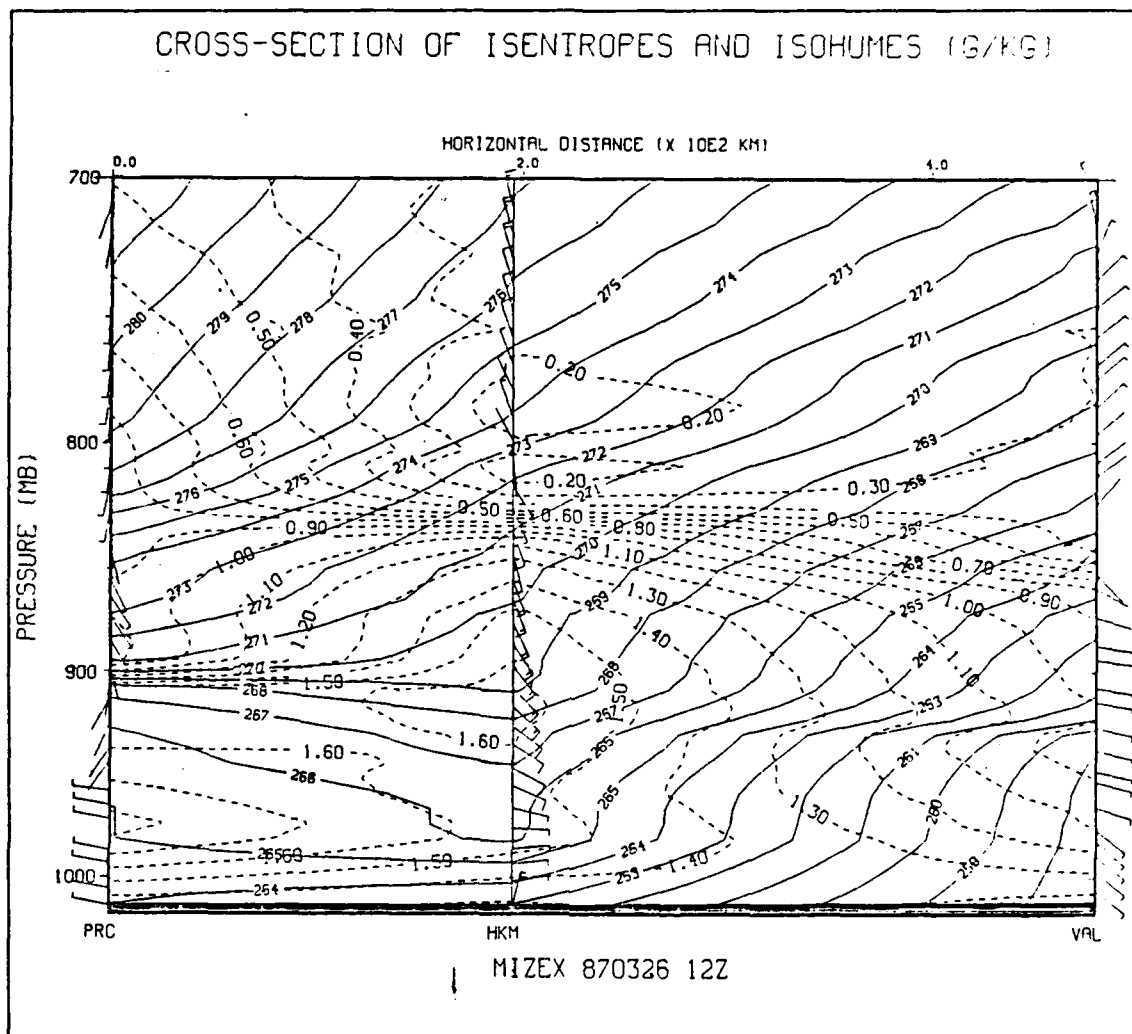


Fig. 14. Cross-section for 12 UTC 26 March 1987: Solid lines are θ in $^{\circ}\text{K}$. Dashed lines are q in g/kg. (PRC = Polar Circle, HKM = Haakon Mosby, VAL = Valdivia)

Below the inversion the layer appears well mixed, but the wind shift at the inversion is much weaker, with southeasterly winds extending to 700mb.

At the Haakon Mosby, the sharp dip in the isentropes noted earlier is between 860mb and 970mb, and appears associated with a region of strong winds in the layer. A wind shift at 860mb from southeasterly to southwesterly is noted, but the shift is not associated with any temperature inversion or moisture gradient. Further aloft, another wind shift occurs near 740mb associated with a weak inversion that has formed at this

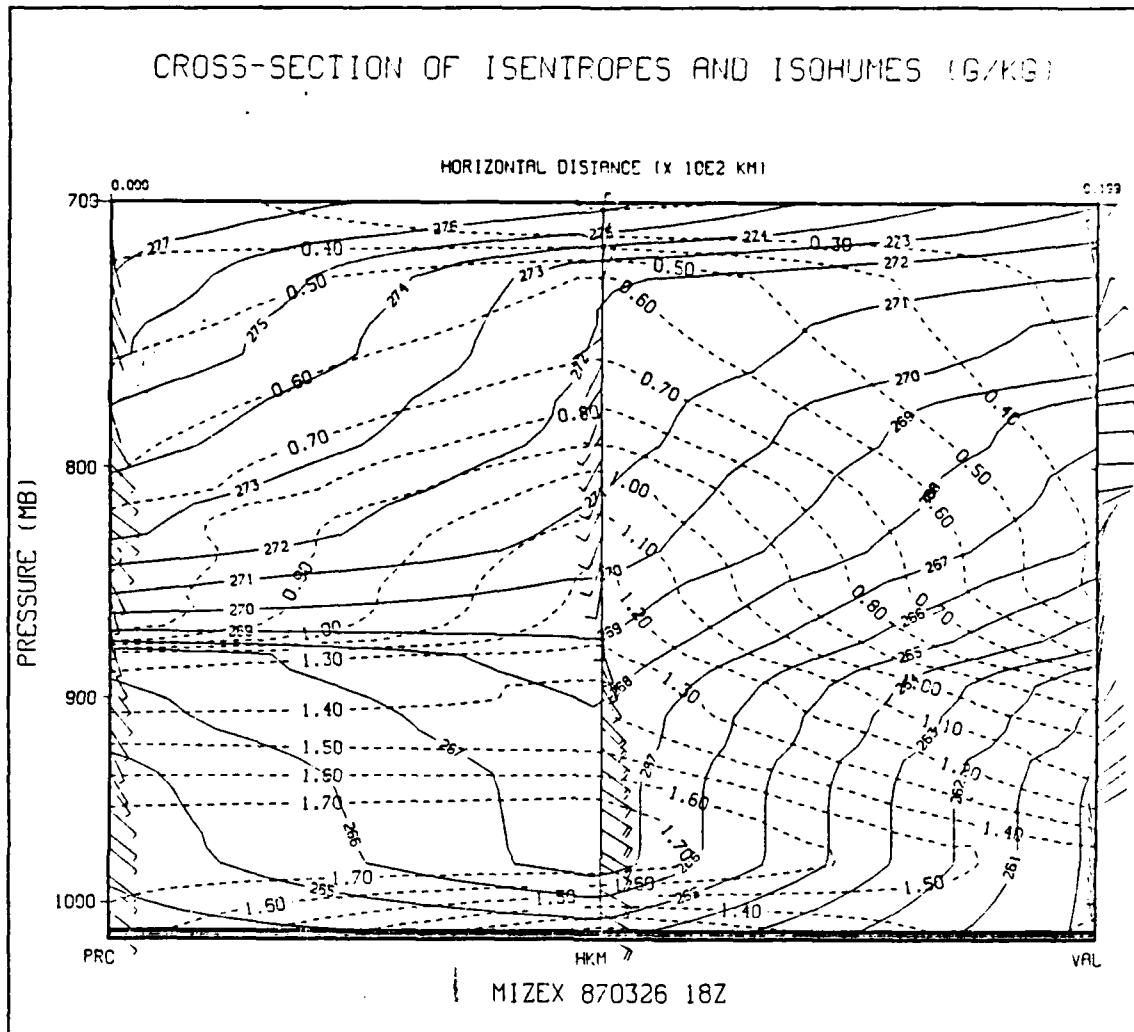


Fig. 15. Cross-section for 18 UTC 26 March 1987: Parameters as in Fig. 14

level. At the Valdivia the temperature profile is similar to that previously described, but the strong moisture gradients noted earlier have dissipated.

Overall, this later spatial cross-section shows two major changes in the lower atmosphere due to continued frontal movement and easterly winds across the Fram Strait. First, the strong slope in the isentropes noted at 12 UTC has flattened considerably. Second, the very strong gradients in moisture noted around 850mb have dissipated. This indicates that the characteristic features of the boundary layer front and polar air mass have weakened considerably, and that the front is beginning to dissipate.

This is due to the strong heat and moisture fluxes over the open ocean causing rapid modification of the polar air mass.

Fig. 16 shows a cross-section observed at 12 UTC 27 March, 18 hours after the establishment of on-ice flow. The positions of the ships for this later cross-section are shown in Fig. 17. Most striking is the absence of strong gradients of temperature or moisture in the boundary layer. A deep well-mixed layer extends to 850mb (1400m) at the Polar Circle with no temperature inversion present. A moderate moisture gradient occurs near 880mb, below a wind reversal near 820mb. A weak inversion is noted near 730mb (2700m). At the Haakon Mosby the mixed layer extends to 900mb (800m) and is capped by a weak subsidence inversion. A wind reversal from southeasterly to northwesterly occurs at 850mb.

A mixed layer extending to 870mb was observed at the Valdivia, the southernmost ship in the section. This mixed layer was capped by a weak subsidence inversion. The vertical wind profile recorded by this radiosonde shows light and variable winds from northwest and north throughout the lower atmosphere, although southeast winds were still recorded at the surface. The remainder of the off-ice wind period was characterized by deep, moist mixed layers capped by weak, high inversions.

To contrast features observed in spatial cross-sections, Fig. 18 shows a single ship time-section observed at the Polar Circle. In the time-sections presented, the time axis increases from left to right. The use of a time-section provides another view of modification of the boundary layer with the onset of on-ice winds. The inversion noted near 900mb at 12 UTC 26 March rises rapidly and is destroyed with passage of the front and establishment of on-ice winds. By 18 UTC 27 March the on-ice flow regime has stabilized, and a weak inversion has formed near 730mb. That inversion caps a mixed layer that has deepened from 800m to nearly 2500m in the 24 hours since the shift to on-ice winds, which is a significant change in the boundary layer. The time-section also shows an overall trend towards decreasing temperatures in the upper boundary layer, with a decrease of nearly 11 K at 800mb during the 30-hour period shown in Fig. 18.

Another interesting feature evident in this time-section is the weakening of the vertical temperature gradient at mid-levels during frontal passage (between 18 UTC 26 March and 06 UTC 27 March). This feature is similar to the dip in the isentropes seen in the cross-sections of 12 UTC and 18 UTC 26 March (Fig. 14 and Fig. 15). From the surface to 860mb a warming trend is evident prior to frontal passage, increasing nearly 4 K at the surface. This is associated with a strong increase in specific humidity from 1.4 g kg to 3.0 g kg near the surface. Above 860mb, the temperatures drop rapidly

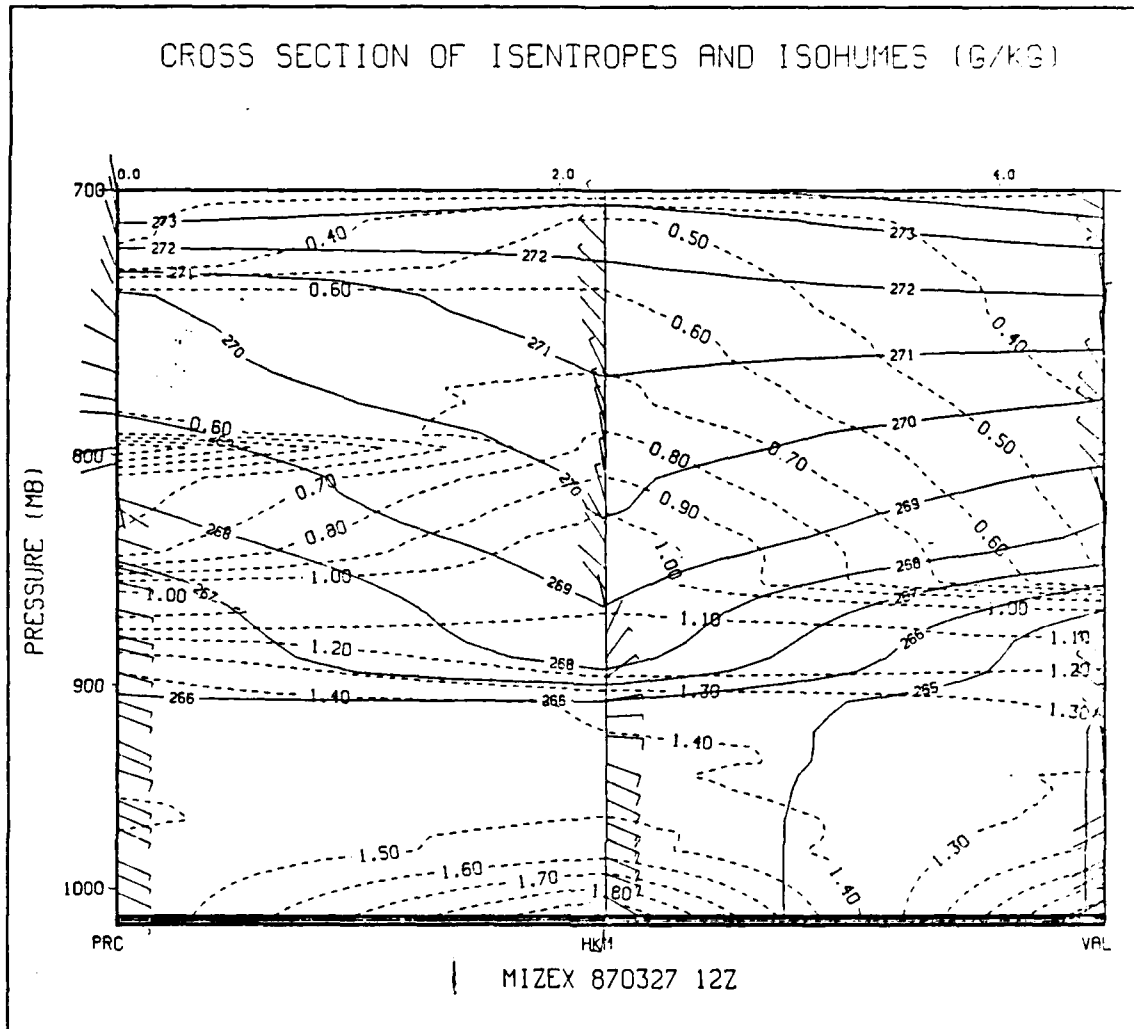


Fig. 16. Cross-section for 12 UTC 27 March 1987: Parameters as in Fig. 14

during the same time interval. After passage and dissipation of the front (06 UTC to 12 UTC 27 March), the vertical temperature gradient increases again, with decreasing temperatures and drying near the surface and dropping temperatures aloft. This feature may be indicative of increased turbulence due to buoyancy forces in addition to mechanical turbulence in the thick clouds associated with the front. The increase in lower-level moisture appears to be related to the increasing temperatures at the surface during frontal passage.

Clearly, both dynamic and thermodynamic processes were important to the development of observed features during this frontal passage. The dynamic processes

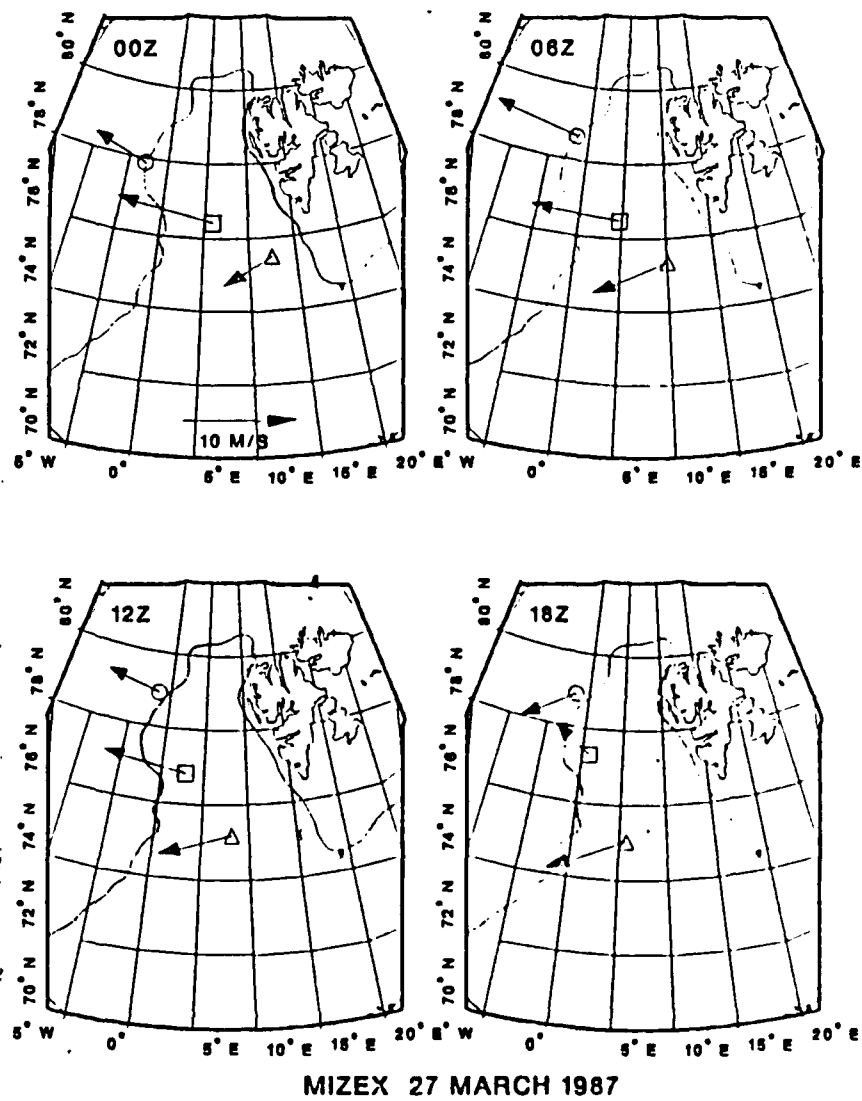


Fig. 17. Ship positions for 27 March 1987, with vector surface winds: Polar Circle = \circ , Haakon Mosby = \diamond , Valdivia = ∇

front led to rapid lifting and destruction of inversion layers. Continued on-ice flow allowed modification of the air mass by strong heat and moisture fluxes due to the open ocean. This resulted in a MABL with a deep, moist mixed layer capped by high, weak inversions, characteristic of a near neutral MABL, as it flowed onto the MIZ.

2. Off-ice flow

An off-ice flow regime in the MIZEX area occurred from 00 UTC 4 April to 06 UTC 5 April 1987. Fig. 19 presents the sea-level pressure analysis observed at 12 UTC 4 April. Synoptic forcing was due to formation and movement of a cyclone south of the MIZ, and establishment of pressure gradients favorable to off-ice flow in the region. Fig. 20, the NOAA-10 AVHRR Channel 4 photo taken at 1022 UTC 4 April, shows that the Fram Strait and MIZ are largely obscured due to the cirrus blow-off of the cyclone. Sea-level pressures decreased from 1033mb on 2 April to 1014mb on 4 April, remaining steady during the flow regime. Cloudiness reported by the Polar Circle was 8.8 stratus and fractostratus at 00 UTC 4 April decreasing to 4.8 stratus and fractostratus during 4 April, then increasing to 8.8 stratus on 5 April. Haakon Mosby reported 8.8 stratocumulus decreasing to 5.8 stratocumulus from 15 UTC to 18 UTC 4 April, then a rapid increase to 8.8 stratocumulus by 00 UTC 5 April.

The positions of the ships during off-ice flow are shown with vector surface winds in Fig. 21. Both the Polar Circle and the Haakon Mosby were located at or near the ice edge during the regime within 80 km of each other. The Valdivia departed the experiment area on 3 April and was no longer recording data. Due to the small number of ships in the area, time-sections of the sounding data proved the only useful means of data display.

A single ship time-section observed at the Polar Circle is presented in Fig. 22. Parameters are as previously described for Fig. 14, with the time axis increasing from left to right. The associated rawinsonde profiles are shown in Fig. 23. Prior to the establishment of off-ice flow on 4 April, winds at the Polar Circle veered from easterly (06 UTC 3 April) to westerly (18 UTC 3 April) due to passage of the synoptic-scale low to the south, and have diminished from 5 m/s to less than 2.5 m/s. This is accompanied by rapidly decreasing temperatures near the surface. Polar Circle reported a decrease in temperature from -4°C to -11°C associated with this wind shift. A very strong surface based inversion developed during this period, with both temperature and specific humidity increasing with height. Above the surface inversion, temperatures assume a stable lapse rate. Moisture is initially smoothly distributed from the inversion to 700mb. However, a strong moisture gradient appears aloft near 730mb, lowering in height and

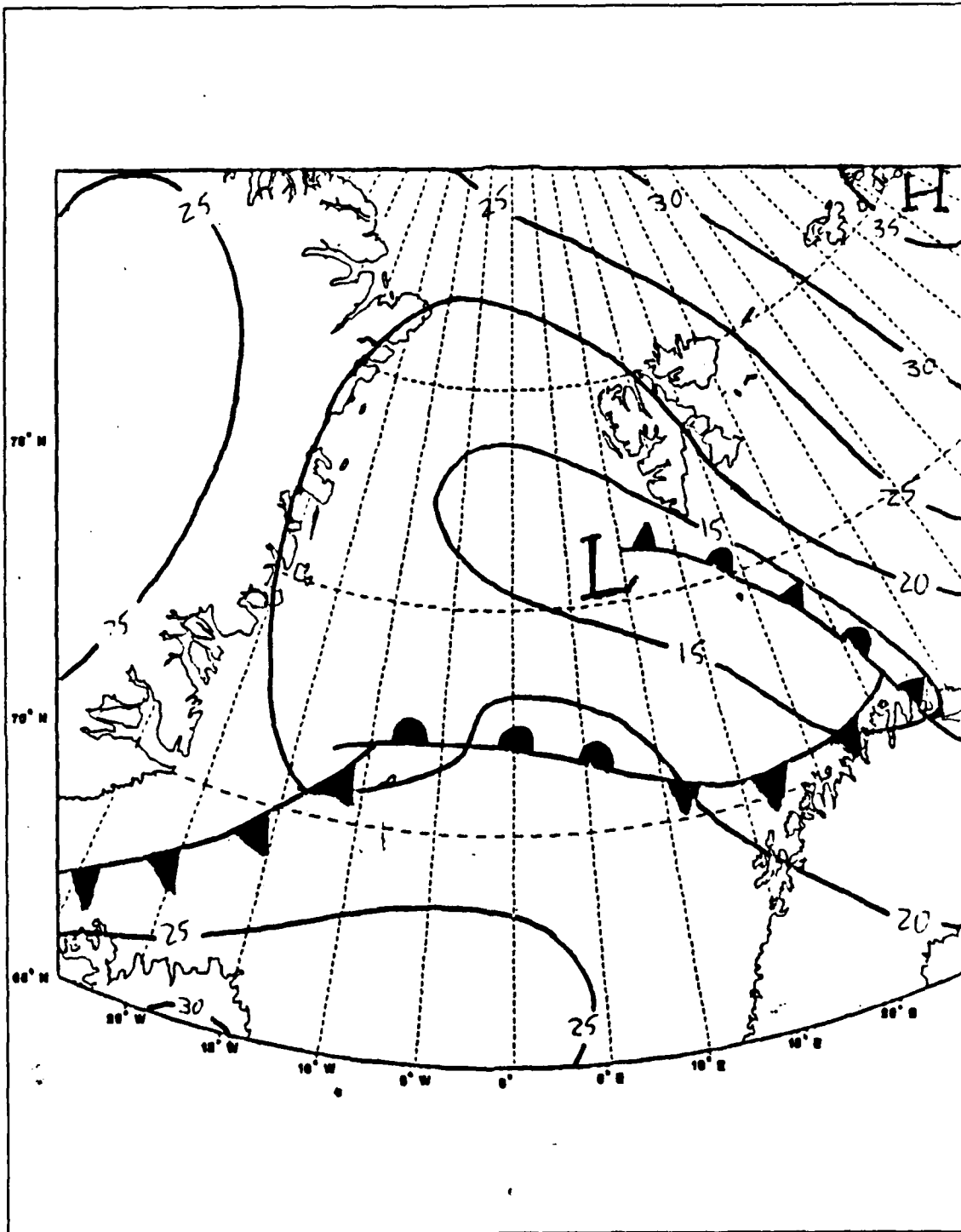


Fig. 19. Sea-level pressure analysis for 12 UTC 4 April 1987.



Fig. 20. NOAA-10 AVHRR photo for 1022 UTC 4 April 1987.

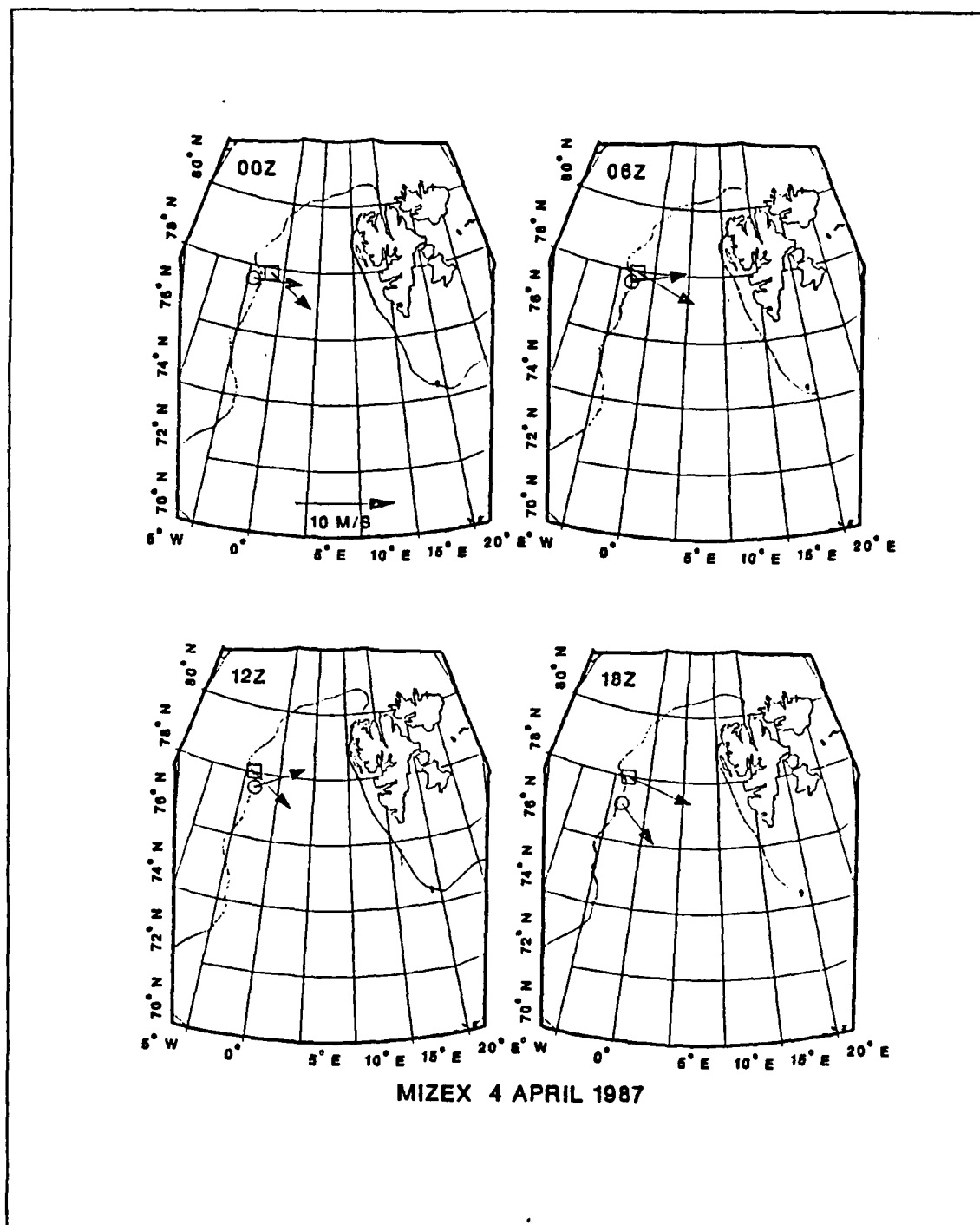


Fig. 21. Ship positions for 4 April 1987, with vector surface winds: Polar Circle = \circ , Haakon Mosby = \diamond .

intensifying to around 800mb by 00 UTC 4 April. This may indicate increasing subsidence in the region.

By 00 UTC the off-ice regime is well established at the Polar Circle, and winds have increased slightly to above 2.5 m s. This has caused the surface based inversion to lift, rising to 860mb, and becoming coincident with the moisture gradient. This initial inversion layer continues to rise and weaken, becoming a broad stable layer between 900mb and 800mb by 18 UTC 4 April. The moisture gradient due to subsidence continues to drop, stabilizing near 900mb by 18 UTC.

The trend towards decreasing surface temperatures has continued during this period. The Polar Circle reported a further decrease from -11°C to -17°C by 12 UTC 4 April. This is accompanied by the formation of a second surface inversion between 00 UTC and 12 UTC. This second inversion also rises from the surface during continued off-ice flow, settling near 970mb coincident with an increasing moisture gradient. From 12 UTC 4 April to 06 UTC 5 April, the inversion caps a very thin well-mixed layer from the surface to 980mb.

The single ship time-section observed at the Haakon Mosby during off-ice flow is shown in Fig. 24, with parameters as in Fig. 14. The associated rawinsonde profiles are shown in Fig. 25. The Haakon Mosby time-section and rawinsondes have features similar to those seen at the Polar Circle. From 12 UTC to 18 UTC 3 April, prior to the establishment of off-ice flow, Haakon Mosby recorded strong southeasterly flow, with no inversions or strong moisture gradients noted from the surface to 700mb. A rapid shift in winds from southeasterly to westerly along with dropping wind speeds occurred between 18 UTC 3 April and 00 UTC 4 April. This was associated with rapidly dropping temperatures at the surface (-3°C to -16°C during the period) and the development of a strong surface based inversion extending to 980mb. A second inversion is noted near 960mb. A sharp decrease in upper-level moisture by 00 UTC is again associated with increasing subsidence aloft in the region.

By 06 UTC 4 April, the two inversions noted at 00 UTC have lifted and stabilized. The lower inversion is located near 960mb, and caps a layer of sharply decreasing specific humidity towards the surface. The second, upper inversion, is located near 850mb coincident with a decreasing moisture gradient due to subsidence. Between the two inversions is a relatively moist layer well-mixed in temperature. A wind shift near 850mb is associated with the upper inversion throughout the period. This condition persisted until the end of the off-ice flow regime at 06 UTC 5 April.

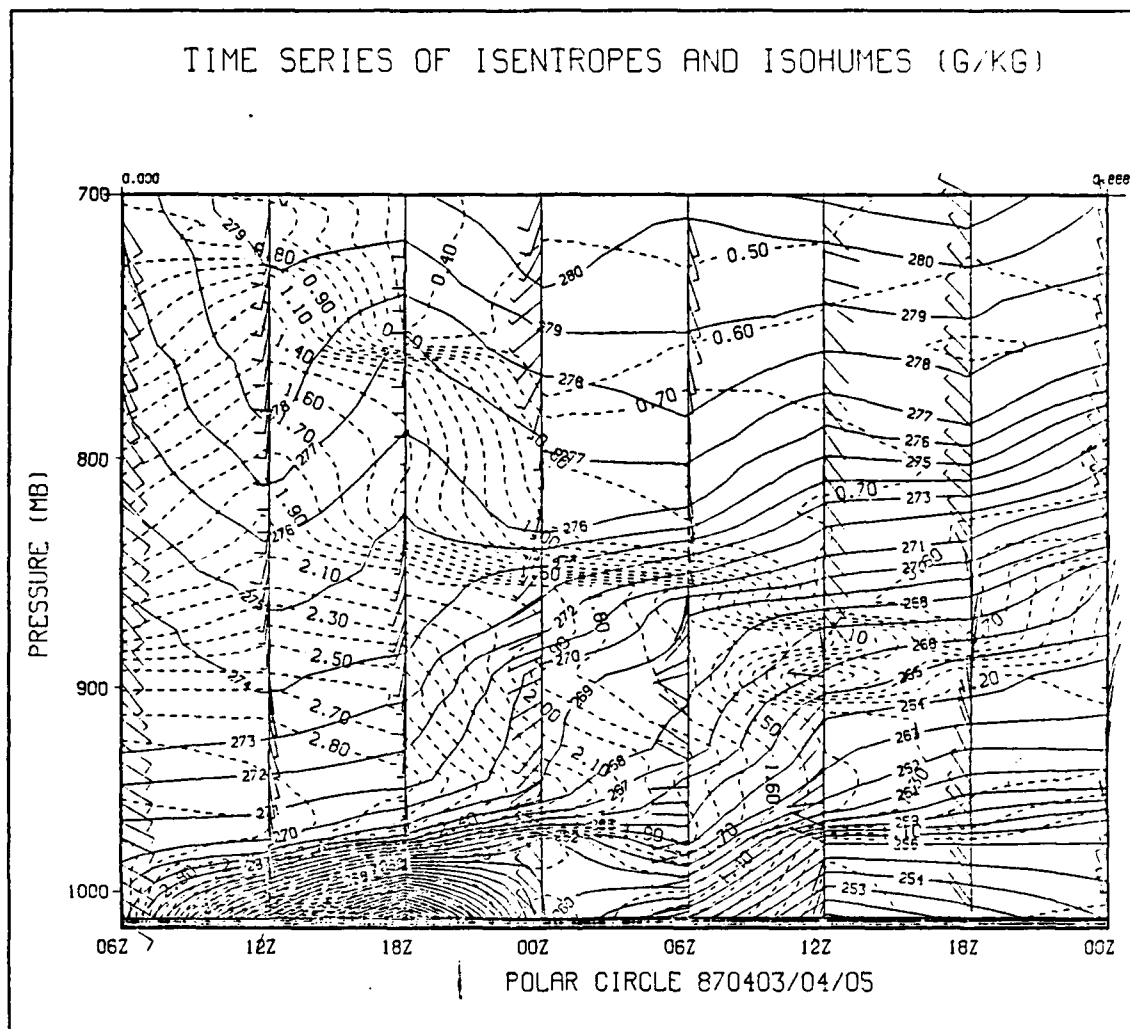


Fig. 22. Time-section of Polar Circle radiosondes for 3/4 April 1987: Parameters as in Fig. 14.

Common features were observed at both ships during this off-ice case. Onset of the off-ice flow was accompanied by rapidly dropping temperatures at the surface and development of surface based inversions. Continued off-ice flow resulted in lifting and splitting of the surface inversions creating dry regions near the surface and aloft, with a relatively moist region between the two inversions. Several factors may contribute to formation of the observed features during this flow regime. The ABL encounters increased heat flux at the ice edge causing increased convective turbulence and decreasing stability. However, increased surface roughness at the MIZ would increase mechanical

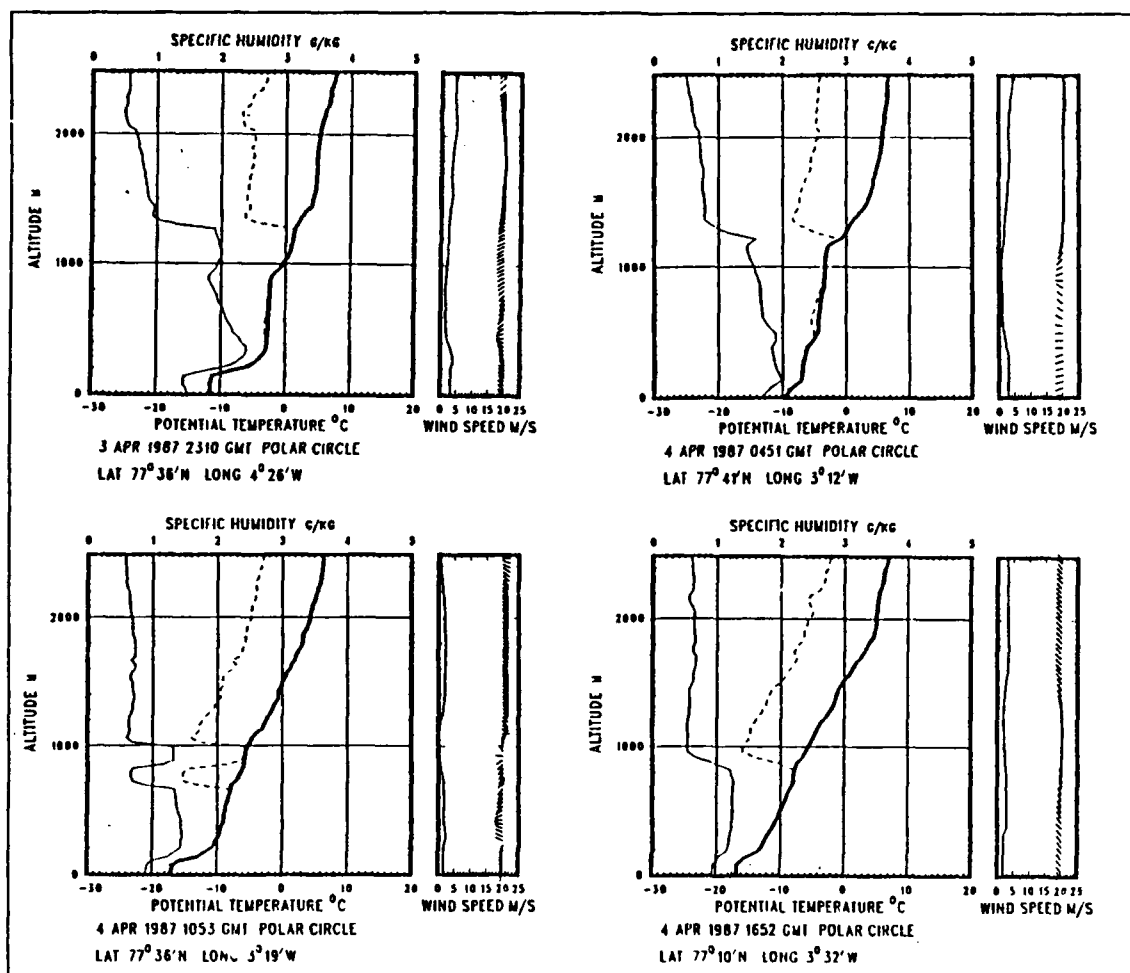


Fig. 23. Polar Circle rawinsonde profiles for 4 April 1987: Parameters as in Fig. 11.

turbulence as well. It is difficult to assess the relative importance of each without increased spatial resolution of the data points.

3. Parallel Flow

A parallel flow regime (northerly flow with ice to the right of the wind) occurred from 00 UTC 7 April to 06 UTC 8 April. Fig. 26 presents the sea-level pressure analysis for 12 UTC 7 April 1987. Synoptically, the juxtaposition of a stalled low pressure center near Svalbard, a newly developed cyclone south of the MIZ, and a strong high pressure region over Greenland forced northerly winds throughout the Fram Strait/MIZ region. The NOAA-9 AVHRR Channel 4 photo for 0533 UTC 7 April, shown in Fig. 27,

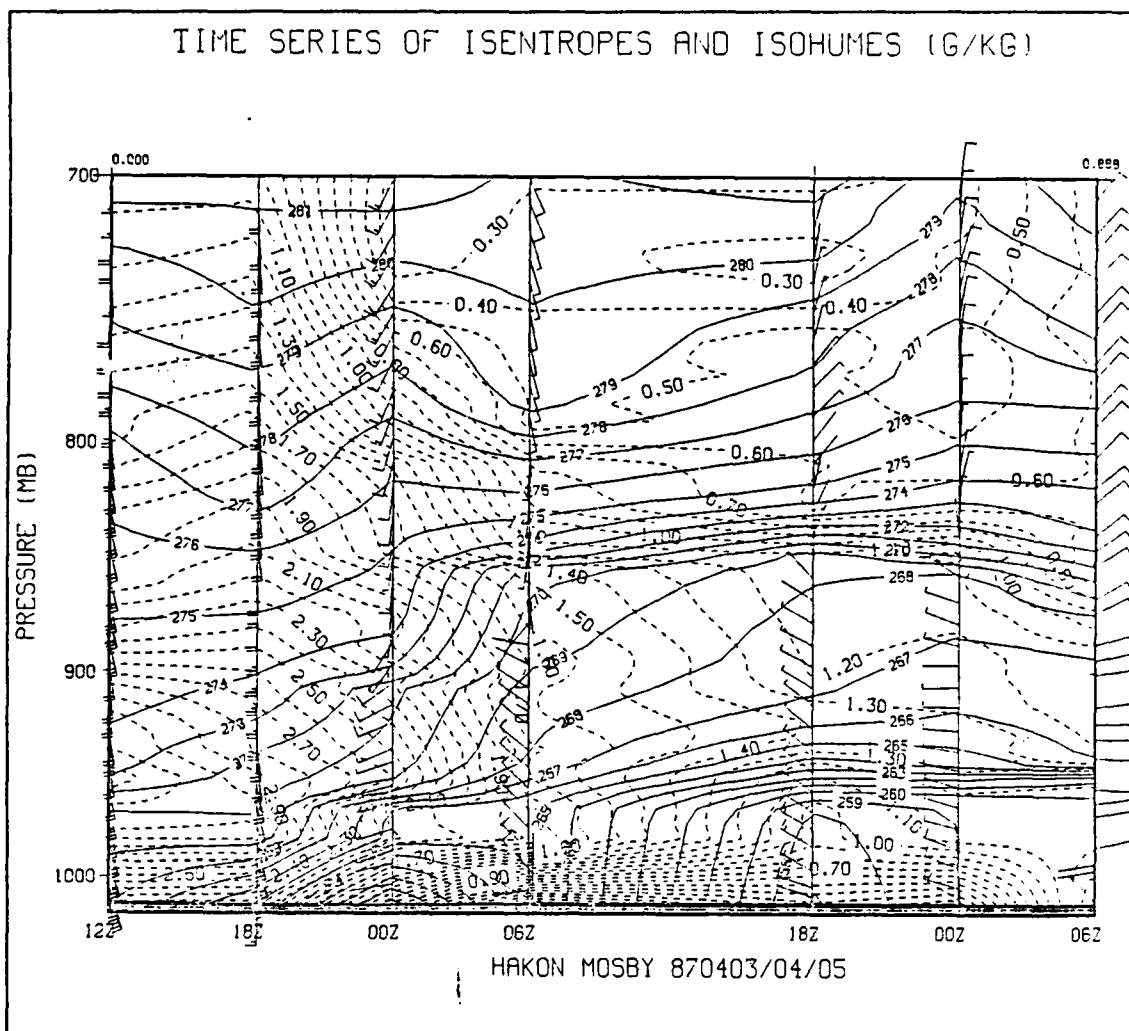


Fig. 24. Time-section of Haakon Mosby radiosondes for 3/4 April 1987: Parameters as in Fig. 14.

clearly shows N - S trending cloud streets indicative of flow along the Greenland Sea MIZ. Average wind speeds of 6.5 m/s and 8.5 m/s were recorded by the Polar Circle and the Haakon Mosby, respectively. Sea-level pressures rose slightly from 1014mb to 1016mb at the Haakon Mosby and from 1016mb to 1018mb at the Polar Circle, indicating the increased influence of the Greenland high. Cloudiness observed by the Polar Circle decreased from 8/8 stratus at 00 UTC 7 April to 1/8 altostratus and cirrus by 00 UTC 8 April, then increasing rapidly to 8/8 stratus by 12 UTC 8 April. Haakon Mosby

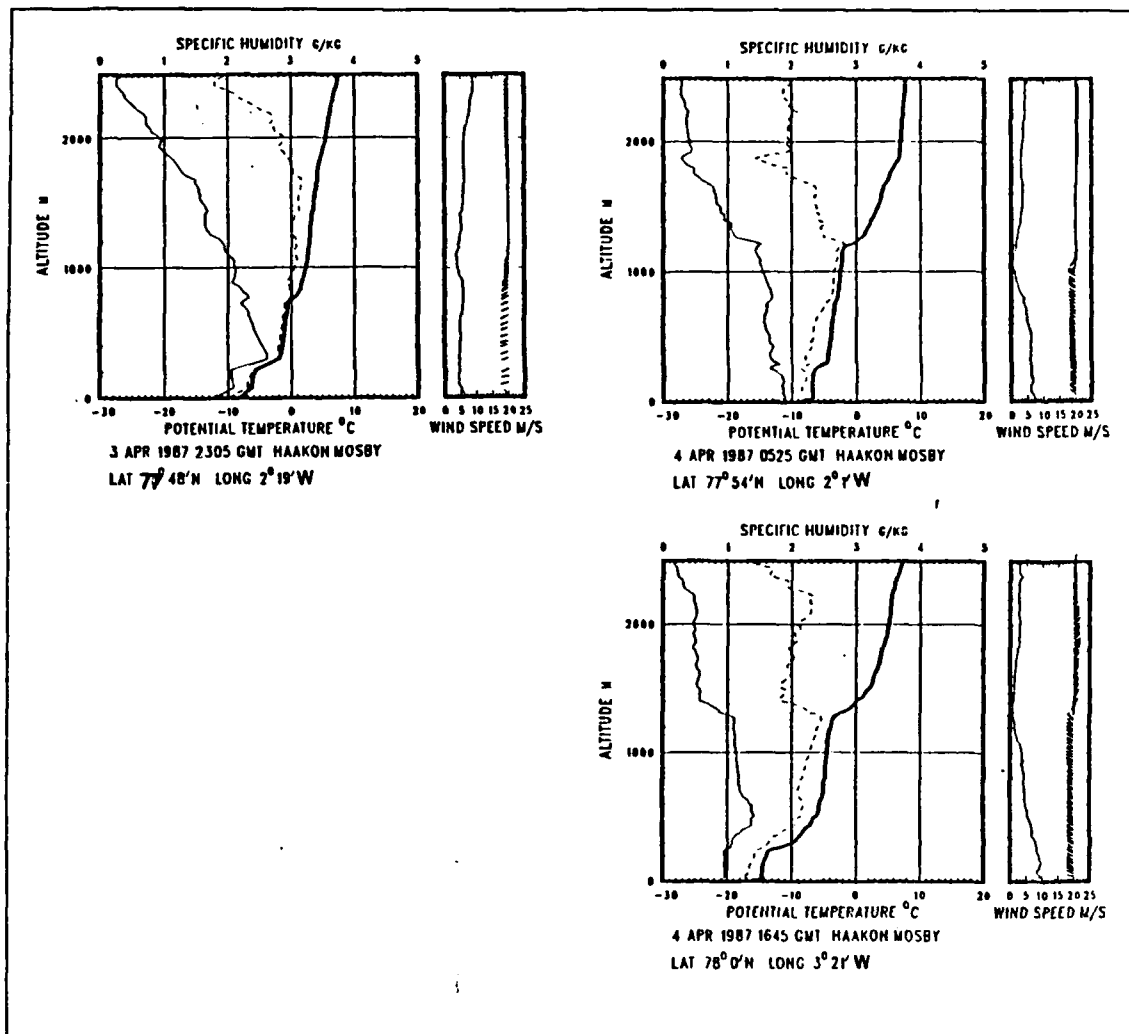


Fig. 25. Haakon Mosby rawinsonde profiles for 4 April 1987: Parameters as in Fig. 11.

reported 6/8 stratus at 00 UTC 7 April decreasing to 2/8 stratocumulus and cumulus by 18 UTC 7 April, then a rapid increase to 6/8 stratus on 8 April.

The position of the ships on 7 April is shown with vector surface winds in Fig. 28. The Polar Circle remained near 77°N 5°W from 7 to 8 April, located well within the ice pack. The Haakon Mosby was located 180 km northeast of the Polar Circle in open ocean. The relative positions of the ships during parallel flow is important because they are in fact sampling different environments. At the Polar Circle, air parcels during parallel (northerly) flow would have trajectories that cross ice only for several

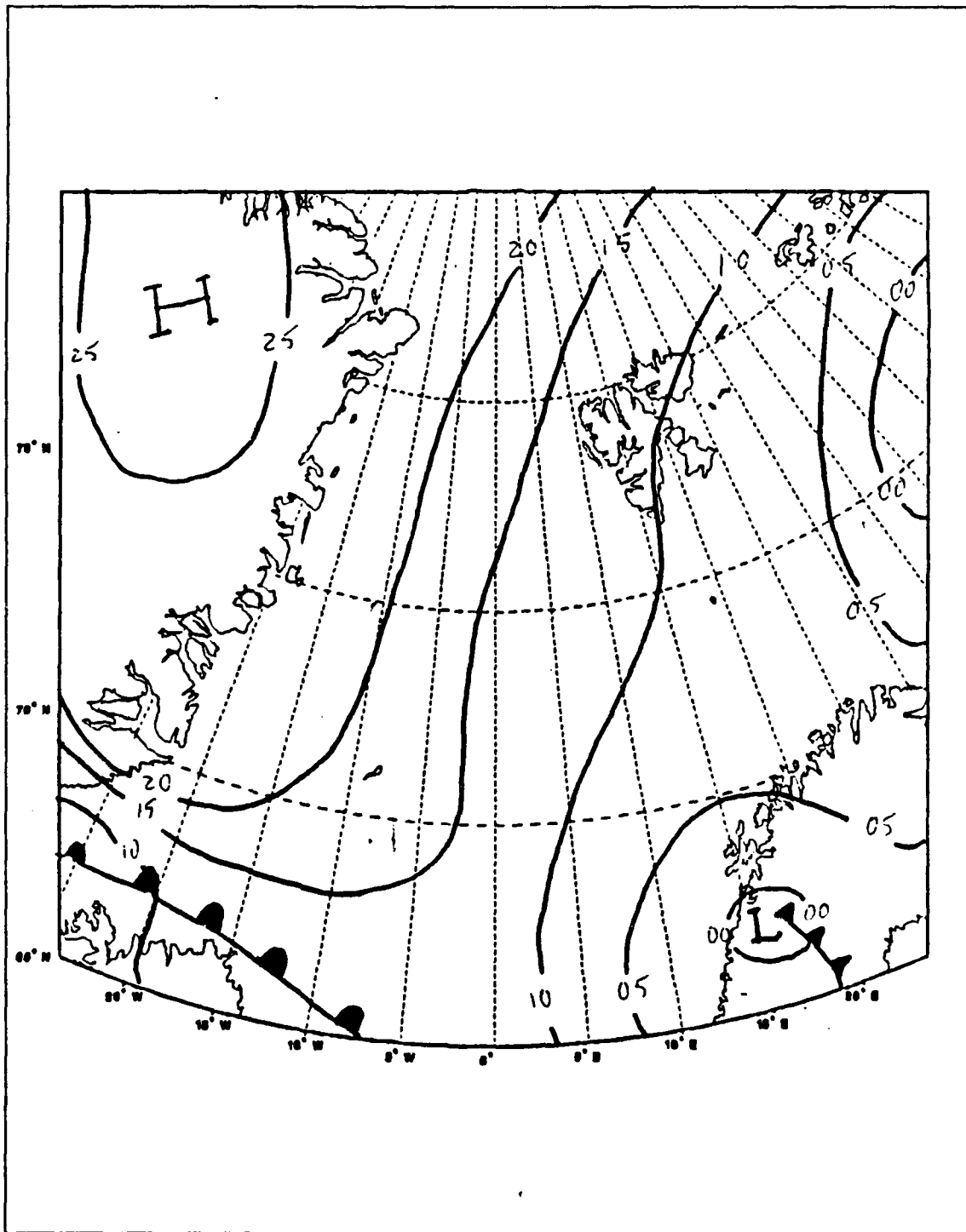


Fig. 26. Sea-level analysis for 12 UTC 7 April 1987.

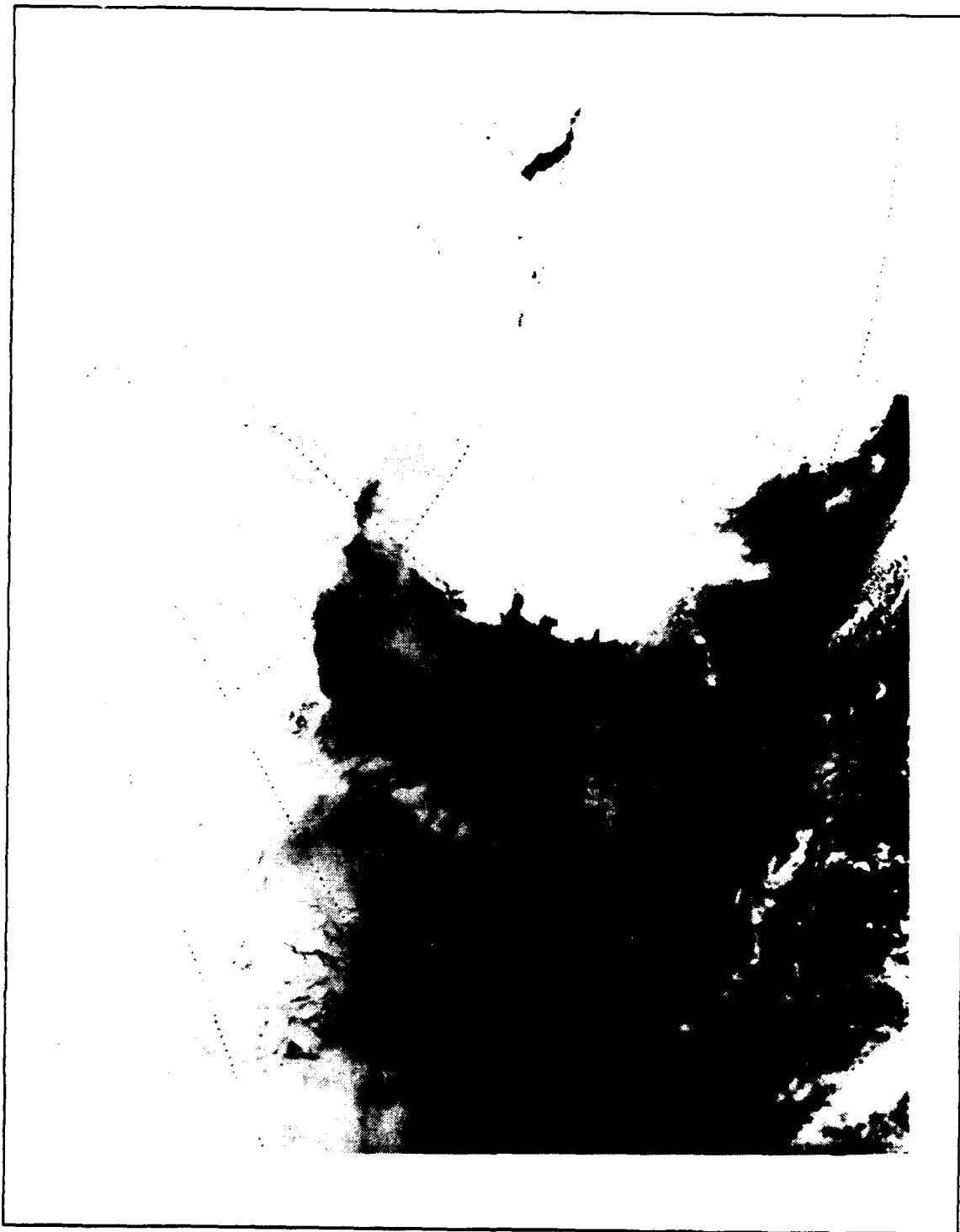


Fig. 27. NOAA-9 AVHRR Channel 4 photo for 0533 UTC 7 April 1987.

hundreds of kilometers prior to measurement. This should cause cooling of the atmosphere due to negative heat flux at the ice surface, and therefore stable ABL conditions. However, at the Haakon Mosby air parcels would flow across an ice edge (off-ice) 100 to 400 km to the north, and would experience modification by the open ocean prior to measurement. These differences are readily noted in the data of each ship.

A single ship time-section observed at the Polar Circle is presented in Fig. 29, with parameters as in Fig. 14. The associated rawinsondes are displayed in Fig. 30. The Polar Circle time-section reveals boundary layer features expected from over-ice trajectories. Just prior to the establishment of parallel flow, relatively warm, moist conditions associated with light easterly (on-ice) flow were observed at the Polar Circle. Between 18 UTC 6 April and 06 UTC 7 April, winds backed from easterly to northerly and increased to 6 m s. A rapid decrease in potential temperature, from 267 K to 259 K, and specific humidity, from 2.3 g kg to 1.3 g kg, occurred at the surface as a result of the wind shift, and a very strong elevated inversion formed near 960mb. Above the inversion, a dry region is noted between 950mb and 900mb, with a strong decrease in moisture above 880mb.

Between 06 UTC and 12 UTC 7 April a slight wind shift from northerly to northeasterly has dramatic effects near the surface. The rapidly decreasing temperatures experienced early in the parallel flow regime are reversed as warmer air advected over the ice, with surface temperatures increasing from 259 K to 263 K associated with an increase in moisture. The strong inversion noted near 960mb weakens considerably and the dry region above it has dissipated. Changes above 900mb due to this short duration wind shift appear minimal.

By 18 UTC 7 April, northerly flow has been re-established, and the rapidly decreasing temperatures due to over ice trajectories continue through 00 UTC. This continued cooling of the ABL causes the formation of a deep surface layer, marked by a surface-based inversion extending to nearly 890mb. Surface temperatures recorded by the Polar Circle during this period of northerly flow reached -20°C ($\theta = 250$ K), the coldest temperature recorded by any ship during MIZEX-87. Formation of the surface inversion is again associated with a dry region from 970mb to 900mb. This dry region remains a significant feature of the boundary layer through 06 UTC 8 April and the end of the flow regime.

A strong elevated inversion is also noted near 830mb at 18 UTC April, marked by sharp gradients in both temperature and moisture. This inversion appears to be a continuation of weak inversion features noted at 06 UTC and 12 UTC, which were

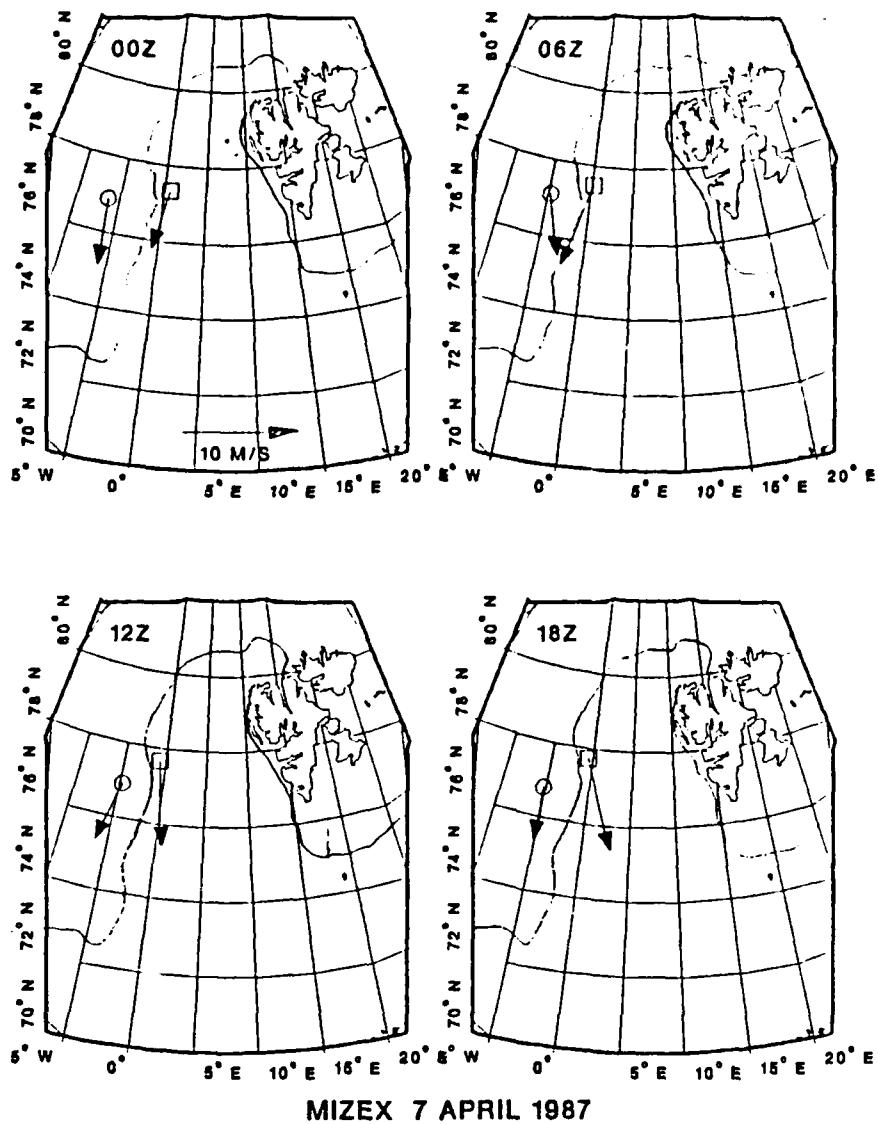


Fig. 28. Ship positions for 7 April 1987, with vector surface winds: Polar Circle = \circ , Haakon Mosby = \diamond .

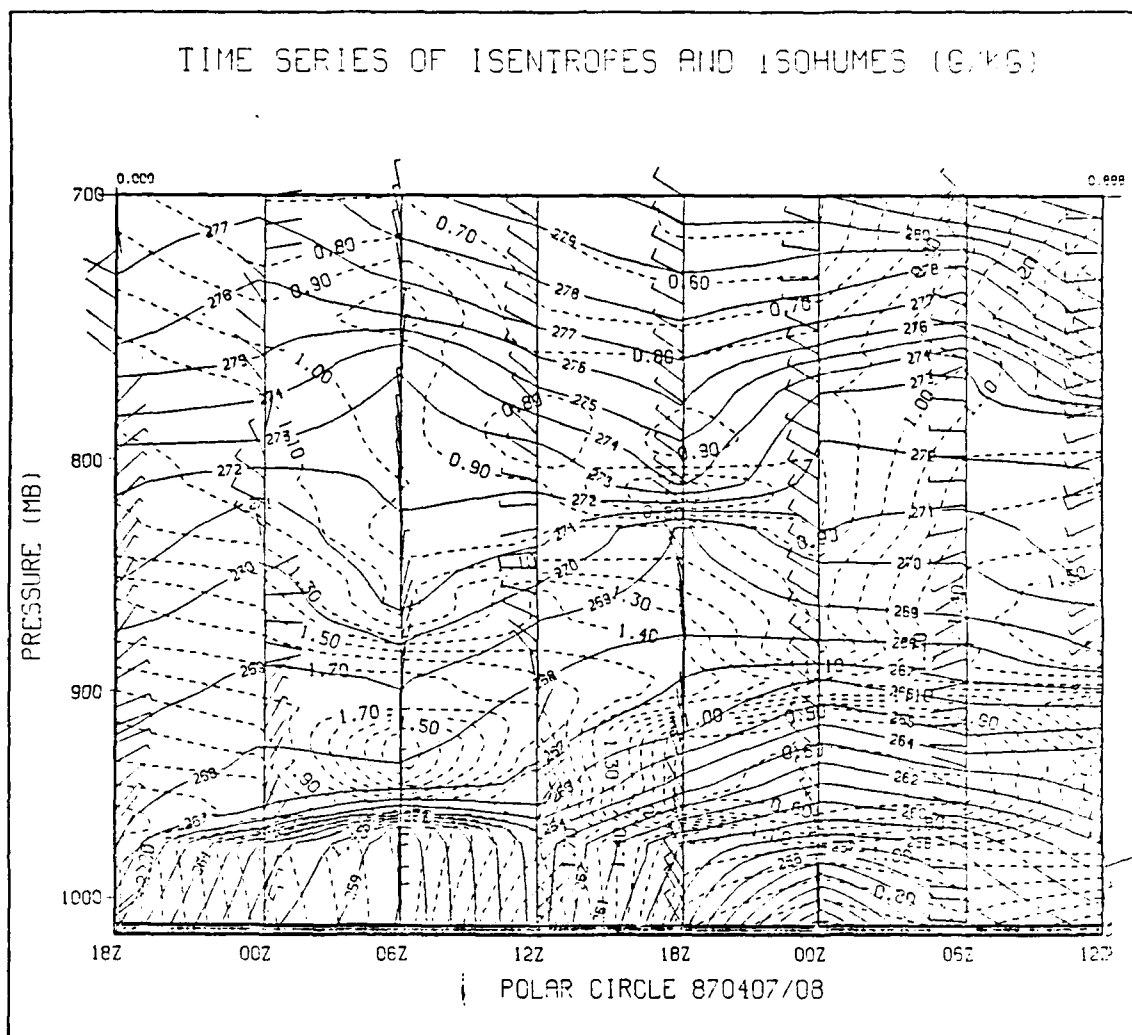


Fig. 29. Time-section of Polar Circle soundings for 7/8 April 1987: Parameters as in Fig. 14.

marked by moisture gradients only. These secondary inversion features appear to parallel development and deepening of the surface layer from 06 UTC to 18 UTC, rising from 890mb to 830mb. This elevated inversion dissappears by 00 UTC 8 April.

Above 800mb, the trend towards rapidly decreasing temperatures at the surface appears offset by a slightly higher temperatures aloft, increasing approximately 2°K from 00 UTC to 18 UTC 7 April. This may be due to increased subsidence from the Greenland high during this period. After 18 UTC, temperatures above 800mb show minor decreases through the end of the flow regime.

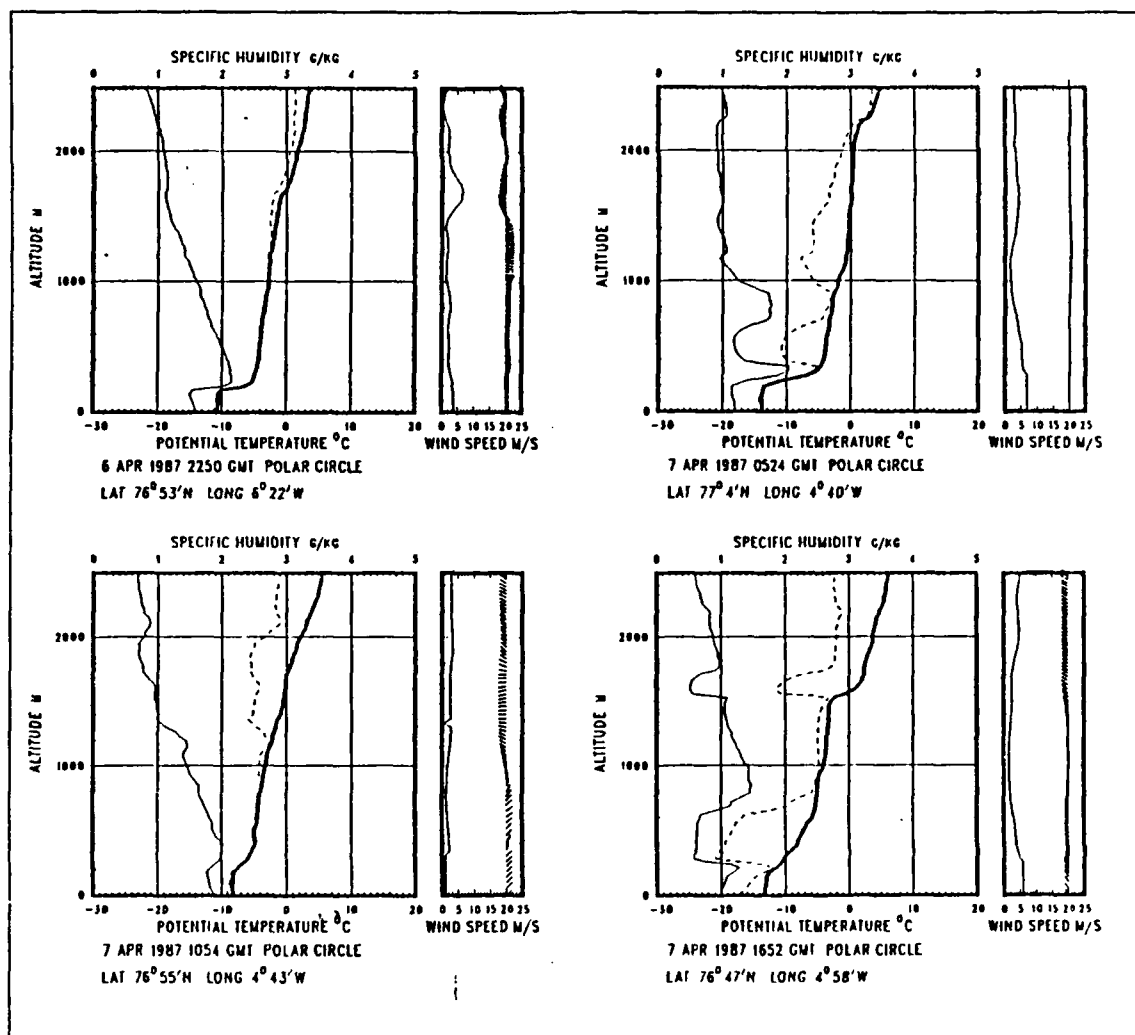
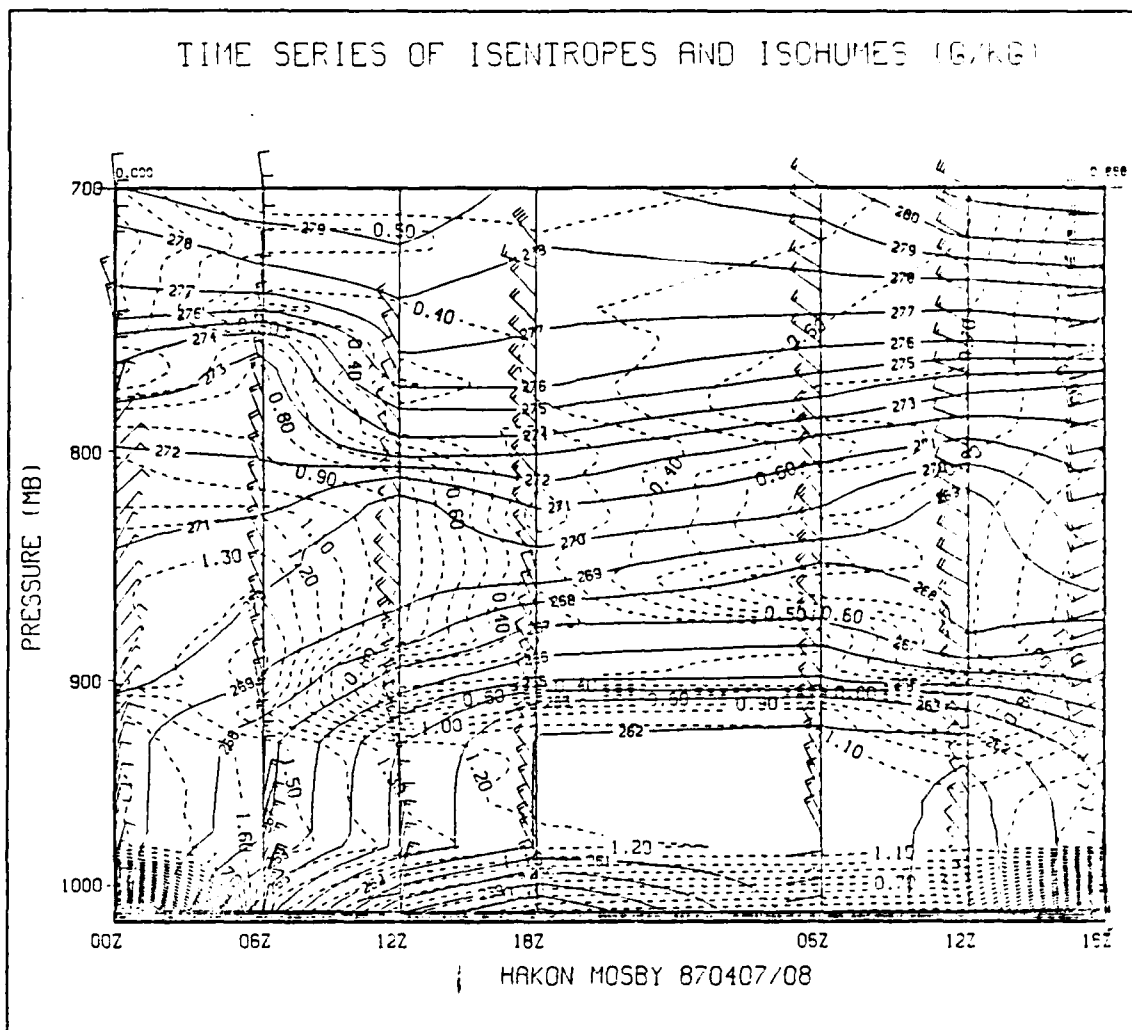


Fig. 30. Polar Circle rawinsonde profiles for 7 April 1987: Parameters as in Fig. 11.

Fig. 31 displays the single ship time-section observed at the Haakon Mosby, with parameters as in Fig. 14. The associated rawinsonde profiles are presented in Fig. 32. The Haakon Mosby time-section shows similar trends of decreasing surface temperatures and weak upper-level temperature increases during the parallel flow regime. However the boundary layer features observed more closely resemble features observed during the off-ice flow discussed earlier, as might be expected considering the air parcel trajectories. The establishment of parallel flow at 00 UTC 7 April is associated



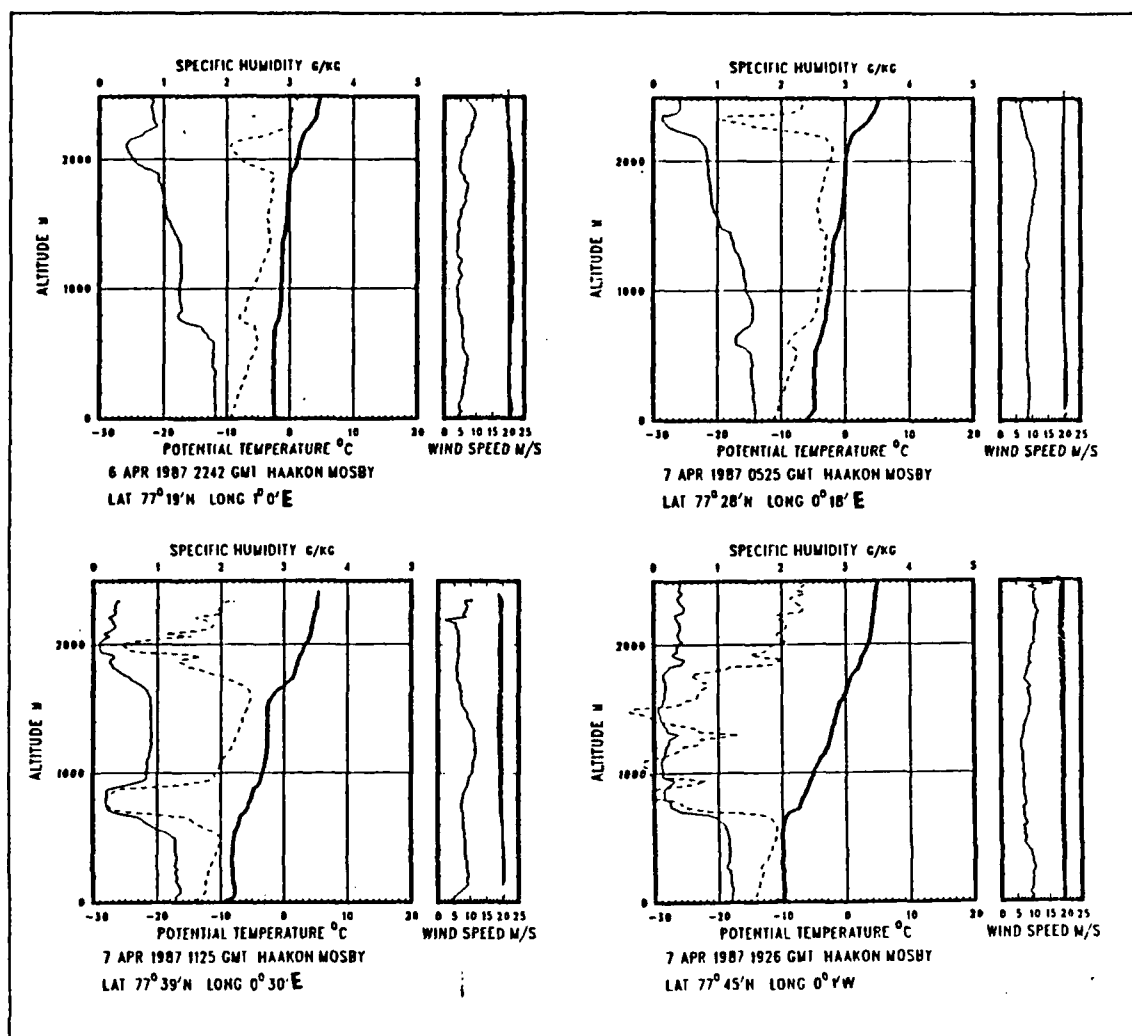


Fig. 32. Haakon Mosby rawinsonde profiles for 7 April 1987: Parameters as in Fig. 11.

to 18 UTC 7 April. The overall structure of the boundary layer at the Haakon Mosby remains constant through the end of the flow regime once parallel flow becomes firmly established.

During the parallel flow case, contrasting features in the ABL were observed at the Polar Circle and Haakon Mosby due to their respective positions. Polar Circle reported development of a strong surface based inversion and elevated inversion features, rapidly decreasing surface temperatures, and several alternating moist and dry layers in the vertical. Formation of multiple elevated inversions with moderately decreasing

surface temperatures were observed at the Haakon Mosby, with development of a moist well-mixed mid-layer with dry regions near the surface and aloft. The multiple surface and elevated inversions and vertical variations in moisture observed at both ships may be indicative of the interleaving of inversions discussed in Guest *et al* (1988). These complex interactions may be due to differential advection caused by local circulation features. Another possibility is layer overturning due to variations in ABL stability across the ice edge. These strong variations in the ABL over the short horizontal scales of the ice edge illustrate the extreme complexity of the ABL under parallel flow conditions.

V. SUMMARY AND RECOMMENDATIONS

A. SUMMARY

The focus of this thesis has been the documentation of boundary layer phenomena in the MIZ resulting from specific flow regimes with respect to the ice edge. This has allowed the examination of specific boundary layer features, such as inversions and mixed layers, as they form and develop under the influence of differing physical processes. Three wind flow regimes were examined: on-ice flow, off-ice flow, and flow parallel to the ice edge.

On-ice flow was preceded by a cold air outbreak and an associated boundary layer front moving rapidly westward across the Fram Strait. Approach and passage of the front resulted in lifting and destruction of inversion layers in the MIZ ABL. Continued on-ice flow showed development of a near-neutral MABL due to oceanic modification of the lower atmosphere. This MABL was characterized by a deep, moist mixed layer capped by high, weak inversion layers.

Onset of off-ice flow resulted in rapidly dropping surface temperatures and the development of surface-based inversions. Continued off-ice flow was associated with lifting and splitting of the surface inversions into multiple low-level inversion features. Specific humidity was highest between the inversions at mid-levels with dry regions near the surface and aloft. In general, stable ABL conditions were experienced in the MIZ.

Parallel flow was characterized by strongly varying ABL conditions across the MIZ. Over the ice, parallel flow resulted in rapidly decreasing surface temperatures and development of deep surface and elevated inversion features, characteristic of a stable ABL. Open-ocean measurements showed development of multiple elevated inversions, with a moist mixed layer between inversions and dry regions near the surface and aloft. The differences in these two ABL regimes only a short distance apart illustrates the extreme complexity of the ABL vertical structure during parallel flow.

In all of the cases examined, the role of synoptic forcing was to establish pressure gradients favorable for the basic flow regimes studied. Within a framework of the various flow regimes, boundary layer processes such as the transport of heat, moisture and momentum along with mesoscale differential advection appeared to be important for development of ABL features.

B. RECOMMENDATIONS

A complete understanding of the unique boundary layer phenomena of the Greenland Sea Fram Strait MIZ will require continued study of more complete data sets. The MIZEX-87 data presented in this thesis is sufficiently detailed to establish basic features of the boundary layer, and to qualitatively discuss the importance of various physical processes. However, emphasis on data collection at mesoscale intervals would provide the detailed data required for quantitative analysis of the unique atmospheric processes associated with the MIZ, and allow determination of their relative importance within the boundary layer. In addition, a more thorough description of this dynamic region will lead to a better understanding of the Arctic as a whole.

LIST OF REFERENCES

- Anderson, R.J., 1987: Wind stress measurements over rough ice during the 1984 Marginal Ice Zone Experiment. *J. Geophys. Res.*, **92**, 6933-6941.
- Buck, A.L., 1981: New equations for computing vapor pressure and enhancement factor. *J. Applied Meteorology*, **20**, 1527-1532.
- Businger, J.A. and W.J. Shaw, 1984: The response of the marine boundary layer to mesoscale variations in sea-surface temperature. *Dyn. Atmos. and Oceans*, **8**, 267-281.
- Fairall, C.W., and R. Markson, 1987: Mesoscale variations in surface stress, heat fluxes, and drag coefficient in the marginal ice zone during the 1983 Marginal Ice Zone Experiment, *J. Geophys. Res.*, **92**, 6921-6932.
- Guest, P.S., and K.L. Davidson, 1987: The effect of observed ice conditions on the drag coefficient in the summer East Greenland Sea marginal ice zone. *J. Geophys. Res.*, **92**, 6943-6954.
- Guest, P.S., and K.L. Davidson, 1988: *MIZEX 87 Meteorology Atlas*, Naval Postgraduate School Report, NPS-63-88-004, Monterey, California, 137 pp.
- Guest, P.S., K.L. Davidson, and C.A. Vaucher, 1988: Atmospheric boundary layer features observed in the spring marginal ice zone. *Preprints from Second AMS Conference on Polar Meteorology and Oceanography*, Madison, Wisconsin, 29-31 March, 1988, pp. 73-74.
- Groters, D.J., 1988: The temporal and spatial variability of the marine atmospheric boundary layer and its effect on electromagnetic propagation in and around the Greenland Sea marginal ice zone. Master Thesis, Naval Postgraduate School, Monterey, California, 111 pp.
- Johnson, D.R., and J.D. Hawkins, 1987: The marginal ice zone experiment: 1987. *European Science Notes*, **41**, 567-570.
- Johnson, G.L., D. Bradley and R.S. Wirnoku, 1984: United States Security Interests in the Arctic. *United States Arctic Interests in the 1980's and 1990's*. Springer-Verlag, New York, 369 pp.
- Johannessen, O.M., 1987: Introduction: Summer marginal ice zone experiments during 1983 and 1984 in Fram Strait and Greenland Sea. *J. Geophys. Res.*, **92**, 6716-6718.
- Kantha, L.H. and G.L. Mellor, 1988: A numerical model of the atmospheric boundary layer over a marginal ice zone. *unpublished*.
- Kellner, G., C. Wamser and R.A. Brown, 1987: An observation of the planetary boundary layer in the marginal ice zone. *J. Geophys. Res.*, **92**, 6955-6965.

- Lenschow, D.H., 1986: Introduction, *Probing the Atmospheric Boundary Layer*, D.H. Lenschow, Ed., Amer. Meteor. Soc., Boston, 1-3.
- Merbs, A., 1988: Petroleum industry research in Arctic and subarctic frontier areas. *Arctic Research of the United States*, 2, 24-26.
- Overland, J.E., R.M. Reynolds and C.H. Pease, 1983: A model of the atmospheric boundary layer over the marginal ice zone. *J. Geophys. Res.*, 88, 2836-2840.
- Overland, J.E., 1985: Atmospheric boundary layer structure and drag coefficients over sea ice. *J. Atmos. Sci.*, 42, 9029-9049.
- Overland, J.E., 1988: A model of the atmospheric boundary layer over sea ice during winter. Print, Second conference on Polar Meteorology and Oceanography, Amer. Meteor. Soc., March 29-31, 1988, Madison, Wisconsin, 69-72.
- Petterssen, S., W.C. Jacobs, and B.C. Haynes, 1956: *Meteorology of the Arctic*. Naval Operations for Polar Projects (OP-03A3), Washington DC, 207 pp.
- Sater, J.E., A.G. Ronhovde, and L.C. Van Allen, 1971: *Arctic Environment and Resources*. The Arctic Institute of North America, Washington DC, 309 pp.
- Schultz, R.R., 1987: Meteorological Features During the Marginal Ice Zone Experiment from 20 March to 10 April 1987, Master Thesis, Naval Postgraduate School, Monterey, California, 86 pp.
- Shapiro, M.A., and L.S. Fedor, 1986: The Arctic Expedition, 1984: Research aircraft observations of fronts and polar lows over the Norwegian and Barents Sea. Part 1. *POLAR LOWS PROJECT Technical Report No. 20*, 56 pp.
- Stewart, R.W., 1979: *The Atmospheric Boundary Layer*. World Meteorological Organization No. 523, 44 pp.
- Vowinkel, E. and S. Orvig, 1970: The climate of the North Polar Basin. *World Survey of Climatology: Vol. 14, Climates of the Polar Regions*, S. Orvig, Ed., Amsterdam, Elsevier, 129-252.
- Willis, Z.S., 1987: The Spatial and Temporal Variability of the Arctic Atmospheric Boundary Layer and Its Effect on Electromagnetic (EM) Propagation, Master Thesis, Naval Postgraduate School, Monterey, California, 108 pp.
- Wyngaard, J.C., 1973: On surface layer turbulence. *Workshop on Micrometeorology*, D.A. Haugen, Ed., Boston, Amer. Meteor. Soc., 101-148.
- Westermeyer, W.E., 1984: United States Arctic Interests: Background for Policy. *United States Arctic Interests in the 1980's and 1990's*. Springer-Verlag, New York, 369 pp.

INITIAL DISTRIBUTION LIST

		No. Copies
1.	Defense Technical Information Center Cameron Station Alexandria, VA 22304-6145	2
2.	Library, Code 0142 Naval Postgraduate School Monterey, CA 93943-5002	2
3.	Chief of Naval Research 800 N. Quincy Street Arlington, VA 22217-5000	1
4.	Oceanographer of the Navy Naval Observatory 34th and Massachusetts Avenue NW Washington, DC 20390-5000	1
5.	Commander Naval Oceanography Command NSTL, MS 39522-5000	1
6.	Commanding Officer Fleet Numerical Oceanography Center Monterey, CA 93943-5005	1
7.	Chairman, Code 63Rd Department of Meteorology Naval Postgraduate School Monterey, CA 93943-5000	1
8.	Chairman, Code 68Co Department of Oceanography Naval Postgraduate School Monterey, CA 93943-5000	1
9.	Professor P.A. Durkee, 63De Naval Postgraduate School Monterey, CA 93943-5000	1
10.	Professor K.L. Davidson, 63Ds Naval Postgraduate School Monterey, CA 93943-5000	3
11.	LT Karl L. Dinkler, USN 1536 NW 7th Avenue Gainesville, FL 32603	2

12. Commanding Officer
Naval Environmental Prediction
Research Facility
Monterey, CA 93943-5006 1
13. Mr. Robert Fett
Naval Environmental Prediction
Research Facility
Monterey, CA 93943-5006 1
14. Chairman, Oceanography Department
U.S. Naval Academy
Annapolis, MD 21402-5000 1
15. Scientific Liaison Office
Office of Naval Research
Scripps Institution of Oceanography
La Jolla, CA 92037-5000 1
16. Library Acquisitions
National Center for Atmospheric Research
P.O. Box 3000
Boulder, CO 80307-5000 1
17. Commanding Officer
Naval Oceanographic Office
NSTL Station
Bay St. Louis, MS 39522 1
18. Commanding Officer
Naval Ocean Research and Development Activity
NSTL Station
Bay St. Louis, MS 39522 1
19. Office of Naval Research (Code 420)
Naval Ocean Research and Development Activity
800 North Quincy Street
Arlington, VA 22217 1
20. Commander
Naval Ocean Systems Center
San Diego, CA 92152 1
21. Commander
Naval Sea Systems Command
Washington D.C. 20362 1
22. LT Zdenka S. Willis
Naval Polar Oceanography Center
4301 Suitland Road
Washington D.C. 20390-5180 1